(IgG) and IgA with cavity formation in patients with pulmonary tuberculosis," *Clinical and Vaccine Immunology*, vol. 15, no. 3, pp. 544–548, 2008.

[9] U. R. Siddiqi, W. Punpunich, C. Chuchottaworn et al., "Elevated anti-tubercular glycolipid antibody titers inhealthy adults as well as in pulmonary TB patients in Thailand," *The International Journal of Tuberculosis and Lung Disease*. In press.

[10] S. Nabeshima, M. Murata, K. Kashiwagi, M. Fujita, N. Furusyo, and J. Hayashi, "Serum antibody response to tuberculosis-associated glycolipid antigen after BCG vaccination in adults," *Journal of Infection and Chemotherapy*, vol. 11, no. 5, pp. 256–258, 2005.

[11] S. D. Lawn and G. Churchyard, "Epidemiology of HIV-associated tuberculosis," *Current Opinion in HIV and AIDS*, vol. 4, no. 4, pp. 325–333, 2009.

[12] J. P. Narain and Y. R. Lo, "Epidemiology of HIV-TB in asia," *Indian Journal of Medical Research*, vol. 120, no. 4, pp. 277–289, 2004.

[13] V. Sánchez-Margalet, C. Martín-Romero, J. Santos-Alvarez, R. Goberna, S. Najib, and C. Gonzalez-Yanes, "Role of leptin as an immunomodulator of blood mononuclear cells: mechanisms of action," *Clinical and Experimental Immunology*, vol. 133, no. 1, pp. 11–19, 2003.

[14] T. Uede, Y. Katagiri, J. Iizuka, and M. Murakami, "Osteopontin, a coordinator of host defense system: a cytokine or an extracellular adhesive protein?" *Microbiology and Immunology*, vol. 41, no. 9, pp. 641–648, 1997.

[15] G. J. Nau, G. L. Chupp, J. F. Emile et al., "Osteopontin expression correlates with clinical outcome in patients with mycobacterial infection," *American Journal of Pathology*, vol. 157, no. 1, pp. 37–42, 2000.

[16] G. J. Nau, L. Liaw, G. L. Chupp, J. S. Berman, B. L. M. Hogan, and R. A. Young, "Attenuated host resistance against Mycobacterium bovis BCG infection in mice lacking osteopontin," *Infection and Immunity*, vol. 67, no. 8, pp. 4223–4230, 1999.

[17] Y. Koguchi, K. Kawakami, K. Uezu et al., "High plasma osteopontin level and its relationship with interleukin-12-mediated type 1 T helper cell response in tuberculosis," *American Journal of Respiratory and Critical Care Medicine*, vol. 167, no. 10, pp. 1355–1359, 2003.

[18] R. van Crevel, E. Karyadi, M. G. Netea et al., "Decreased plasma leptin concentrations in tuberculosis patients are associated with wasting and inflammation," *Journal of Clinical Endocrinology and Metabolism*, vol. 87, no. 2, pp. 758–763, 2002.

[19] T. Kishimoto, O. Moriya, J. I. Nakamura, T. Matsushima, and R. Soejima, "Evaluation of the usefulness of a serodiagnosis kit, the determiner TBGL antibody for tuberculosis: setting reference value," *Kekkaku*, vol. 74, no. 10, pp. 701–706, 1999.

[20] A. Zwerling, S. van den Hof, J. Scholten, F. Cobelens, D. Menzies, and M. Pai, "Interferon-γ release assays for tuberculosis screening of healthcare workers: a systematic review," *Thorax*, vol. 67, no. 1, pp. 62–70, 2012.

[21] A. Nienhaus, A. Schablon, C. Le Bâcle, B. Siano, and R. Diel, "Evaluation of the interferon-γ release assay in healthcare workers," *International Archives of Occupational and Environmental Health*, vol. 81, no. 3, pp. 295–300, 2008.

[22] T. Tabuchi, T. Takatorige, Y. Hirayama et al., "Tuberculosis infection among homeless persons and caregivers in a high-tuberculosis-prevalence area in Japan: a cross-sectional study," *BMC Infectious Diseases*, vol. 11, no. 22, 2011.

[23] N. Harada, Y. Nakajima, K. Higuchi, Y. Sekiya, J. Rothel, and T. Mori, "Screening for tuberculosis infection using whole-blood interferon-γ and Mantoux testing among Japanese healthcare workers," *Infection Control and Hospital Epidemiology*, vol. 27, no. 5, pp. 442–448, 2006.

[24] E. Y. Kim, M. S. Park, Y. S. Kim, S. K. Kim, J. Chang, and Y. A. Kang, "Risk factors for false-negative results of QuantiFERON-TB gold in-tube assay in non-HIV-infected patients with culture-confirmed tuberculosis," *Diagnostic Microbiology and Infectious Disease*, vol. 70, no. 3, pp. 324–329, 2011.

[25] M. Matsumoto, T. Tanaka, T. Kaisho et al., "A novel LPS-inducible C-type lectin is a transcriptional target of NF- IL6 in macrophages," *Journal of Immunology*, vol. 163, no. 9, pp. 5039–5048, 1999.

[26] E. Ishikawa, T. Ishikawa, Y. S. Morita et al., "Direct recognition of the mycobacterial glycolipid, trehalose dimycolate, by C-type lectin Mincle," *Journal of Experimental Medicine*, vol. 206, no. 13, pp. 2879–2888, 2009.

[27] I. Matsunaga, T. Naka, R. S. Talekar et al., "Mycolyltransferase-mediated glycolipid exchange in mycobacteria," *Journal of Biological Chemistry*, vol. 283, no. 43, pp. 28835–28841, 2008.

[28] R. Z. Topić, S. Dodig, and I. Zoričić-Letoja, "Interferon-γ and immunoglobulins in latent tuberculosis infection," *Archives of Medical Research*, vol. 40, no. 2, pp. 103–108, 2009.

[29] H. Tezuka, Y. Abe, M. Iwata et al., "Regulation of IgA production by naturally occurring TNF/iNOS-producing dendritic cells," *Nature*, vol. 448, no. 7156, pp. 929–933, 2007.

[30] I. P. Oswald, C. M. Dozois, J. F. Petit, and G. Lemaire, "Interleukin-12 synthesis is a required step in trehalose dimycolate- induced activation of mouse peritoneal macrophages," *Infection and Immunity*, vol. 65, no. 4, pp. 1364–1369, 1997.

[31] R. Reljic, A. Williams, and J. Ivanyi, "Mucosal immunotherapy of tuberculosis: is there a value in passive IgA?" *Tuberculosis*, vol. 86, no. 3-4, pp. 179–190, 2006.

[32] A. Fujita, A. Ajisawa, N. Harada, K. Higuchi, and T. Mori, "Performance of a whole-blood interferon-gamma release assay with mycobacterium RD1-specific antigens among HIV-infected persons," *Clinical and Developmental Immunology*, vol. 2011, Article ID 325295, 2011.

[33] T. Oni, J. Patel, H. P. Gideon et al., "Enhanced diagnosis of HIV-1-associated tuberculosis by relating T-SPOT.TB and CD4 counts," *European Respiratory Journal*, vol. 36, no. 3, pp. 594–600, 2010.

[34] H. L. David, F. Papa, P. Cruaud et al., "Relationships between titers of antibodies immunoreacting against glycolipid antigens from Mycobacterium leprae and M. tuberculosis, the Mitsuda and Mantoux reactions, and bacteriological loads: implications in the pathogenesis, epidemiology and serodiagnosis of leprosy and tuberculosis," *International Journal of Leprosy*, vol. 60, no. 2, pp. 208–224, 1992.

[35] N. Simonney, P. Chavanet, C. Perronne et al., "B-cell immune responses in HIV positive and HIV negative patients with tuberculosis evaluated with an ELISA using a glycolipid antigen," *Tuberculosis*, vol. 87, no. 2, pp. 109–122, 2007.

[36] J. A. Fling, J. R. Fischer Jr, R. N. Boswell, and M. J. Reid, "The relationship of serum IgA concentration to human immunodeficiency virus (HIV) infection: a cross-sectional study of HIV-seropositive individuals detected by screening in the United States Air Force," *Journal of Allergy and Clinical Immunology*, vol. 82, no. 6, pp. 965–970, 1988.

[37] S. Perry, R. Hussain, and J. Parsonnet, "The impact of mucosal infections on acquisition and progression of tuberculosis," *Mucosal Immunology*, vol. 4, no. 3, pp. 246–251, 2011.

[38] C. Ridruechai, S. Sakurada, H. Yanai et al., "Association

between circulating full-length osteopontin and IFN-γ with disease status of tuberculosis and response to successful treatment," *Southeast Asian Journal of Tropical Medicine and Public Health*, vol. 42, no. 4, pp. 876–889, 2011.

[39] H. Chagan-Yasutan, H. Saitoh, Y. Ashino et al., "Persistent elevation of plasma osteopontin levels in HIV patients despite highly active antiretroviral therapy," *Tohoku Journal of Experimental Medicine*, vol. 218, no. 4, pp. 285–292, 2009.

[40] D. D. Taub, A. R. Lloyd, K. Conlon et al., "Recombinant human interferon-inducible protein 10 is a chemoattractant for human monocytes and T lymphocytes and promotes T cell adhesion to endothelial cells," *Journal of Experimental Medicine*, vol. 177, no. 6, pp. 1809–1814, 1993.

[41] H. Chagan-Yasutan, K. Tsukasaki, Y. Takahashi et al., "Involvement of osteopontin and its signaling molecule CD44 in clinicopathological features of adult T cell leukemia," *Leukemia Research*, vol. 35, no. 11, pp. 1484–1490, 2011.

zac00612/zac0915d12z	xppws	S=1	3/30/12	19:59	ArtID: 06062-11	NLM: research-article	CE: MKH

Editor: Ambrose	Section: Biologic Response Modifiers	Designation: T

AAC Journals.ASM.org

Quinolone-Induced Upregulation of Osteopontin Gene Promoter Activity in Human Lung Epithelial Cell Line A549

AQ: A

AQ: au Beata Shiratori,[a] Jing Zhang,[b] Osamu Usami,[a] Haorile Chagan-Yasutan,[a] Yasuhiko Suzuki,[c] Chie Nakajima,[c] Toshimitsu Uede,[d] and Toshio Hattori[a]

Division of Emerging and Infectious Diseases, Graduate School of Medicine, Tohoku University, Sendai, Japan[a]; Research and Development Center, FUSO Pharmaceutical Industries, Ltd., Osaka, Japan[b]; Research Center for Zoonosis Control, Hokkaido University, Sapporo, Japan[c]; and Division of Molecular Immunology, Institute for Genetic Medicine, Hokkaido University, Sapporo, Japan[d]

Quinolones, in addition to their antibacterial activities, act as immunomodulators. Osteopontin (OPN), a member of the extracellular matrix proteins, was found to play a role in the immune and inflammatory response. We found that quinolones significantly enhanced OPN secretion, namely, garenoxacin (220%), moxifloxacin (62%), gatifloxacin (82%), sparfloxacin, (79%), and sitafloxacin (60%). Enhancement of OPN secretion was shown to be due to the effect of quinolones on the OPN gene promoter activity. We also examined the role of quinolones on apoptosis and found that sparfloxacin decreased the late apoptosis of A549 cells, but garenoxacin did not show the antiapoptotic effect. The antiapoptotic effects of quinolones do not appear to be associated with OPN elevation.

Quinolones are synthetic, broad-spectrum antimicrobial agents widely used in clinical and veterinary medicine. They target two essential bacterial enzymes, DNA gyrase and topoisomerase IV (14). Newly developed quinolones especially possess significant *in vivo* bactericidal activity, which makes them attractive therapeutic agents for treatment of tuberculosis, community-acquired pneumonia, and other respiratory tract infections (20). In addition to the bactericidal property, fluoroquinolones (FQs) have been found to elicit an immunomodulatory effect (10).

A number of reports have described the inhibitory effect of FQs on cytokine production. Gatifloxacin (GAT) reduced interleukin-8 (IL-8) release from unstimulated cells of the prostatic cancer cell line PC-3 as well as peptidoglycan-, *Mycoplasma hominis*-, phorbol ester (phorbol myristate acetate [PMA])-, and tumor necrosis factor alpha (TNF-α)-stimulated PC-3 cells but did not significantly reduce the basal level of TNF-α and IL-6 (34). Moxifloxacin (MFX) inhibited IL-8, TNF-α, and IL-1β production in THP-1 cells and in monocytes when preincubated with MFX and stimulated with lipopolysaccharide (LPS) (38). Another report suggested that ciprofloxacin (CIP) may have an immunomodulatory effect on septic patients by attenuating the proinflammatory response, thus decreasing TNF-α, IL-6, IL-1β, and IL-8 levels in patients' serum (15). Levofloxacin at concentrations of 100 μg/ml and higher was found to dose dependently reduce the IL-6 and IL-8 levels in TNF-α-stimulated NL20 human bronchial epithelial cells, but lower concentrations did not alter the studied cytokines (35). Elevated levels of IL-1β, IL-6, and TNF-α in patients with nonbacterial prostatitis became undetectable after treatment with sparfloxacin (SPX) (40).

Several studies attempted to elucidate the signaling pathways and transcription factors that regulate the quinolone-induced cytokine modulation. In A549 cells, IL-1β increased the activities of early intracellular signaling molecules, extracellular signal-regulated kinases 1 and 2 (ERK1/2), phosphorylated Jun N-terminal protein kinase (p-JNK), and NF-κB, whose activities were abrogated by MFX (39). Likewise, in human blood neutrophils, it has been reported that grepafloxacin strongly phosphorylates p38 mitogen-activated protein (MAP) kinase (MAPK) but not p44/42 MAPK or JNK (25).

Osteopontin (OPN), a member of the extracellular matrix proteins, is a multifunctional phosphoprotein that is synthesized by a variety of immune and nonimmune cells (31). Basically, there are three major functions of OPN: involvement in tumorigenesis and metastasis, in mineral metabolism and bone remodeling, and in immune reaction and host defense (36). Because the primary structure and distribution of posttranslational modification are highly conserved among species, it is conceivable that OPN plays an indispensable role in the immune system (8, 9, 32). Within the immune system, OPN is a cytokine secreted by activated T cells, NK cells, dendritic cells, and macrophages (37). In the lung, OPN is expressed by alveolar macrophages and bronchial epithelial cells, the passive physiological barrier of the innate immune system (5, 11, 21). Recently, there is increasing evidence that OPN exists in two isoforms, secreted (sOPN) and/or intracellular (iOPN) protein (36). While sOPN affects the target cell functions by binding to their cell receptors, iOPN binds to MyD88, the downstream protein of the Toll-like receptor (29, 30). Furthermore, it has been reported that OPN binding to CD44v downregulated IL-10 production in macrophages, leading to inhibition of the Th2 immune response, but binding to $\alpha v\beta 3$ integrin receptor led to the expression of IL-12, facilitating the Th1 response (2).

When hosts are insulted by infections, Th1 immunity plays a central role in the elimination of microorganisms, so it is understandable that elevated plasma OPN levels have been found to be associated with tuberculosis and other lung inflammatory diseases (26). OPN deficiency was found to be associated with dissemina-

Received 2 November 2011 Returned for modification 26 December 2011
Accepted 4 March 2012
Published ahead of print ●●●
Address correspondence to Toshio Hattori, hatori286@yahoo.co.jp.

doi:10.1128/AAC.06062-11

tion of mycobacterial disease, and the expression of OPN correlated with an effective immune and inflammatory response and contributed to resistance against mycobacteria in rodents as well as in human (23, 24). OPN also contributed to protection against rotavirus (28), herpes simplex virus type 1 (2, 7), *Listeria monocytogenes* (2), and *Plasmodium falciparum* (19). These reports suggest that OPN plays a role in defense mechanisms against invading microorganisms, including viruses, bacteria, and protozoa.

However, until now, the effect of quinolones on OPN expression in human lung epithelial cells remained to be elucidated. A recent report demonstrated that a human lung type II epithelial cell line (A549) is a suitable model to study host defense cellular responses (18). Therefore, in this study we chose this experimental model to investigate the immunomodulatory effect of CIP, garenoxacin mesylate hydrate (GRN), MFX, GFL, SPF, and sitafloxacin (STF). The antibiotics chosen were CIP and broad-spectrum (SPX), "fourth-generation" (MFX, GAT, STF), and newly developed (GRN) quinolones. This is the first report showing that quinolones enhance OPN production in lung epithelial cells. Because OPN is thought to elicit antiapoptotic effects (6, 17), we investigated whether quinolone-induced OPN production may increase survival in A549 cells.

AQ: B

MATERIALS AND METHODS

Cells. The human A549 alveolar epithelial cell line was obtained from Riken Cell Bank (Tsukuba, Japan). A549/OPN-luc cells were established by cotransfection of pOPN1-luc (42) with puromycin resistance vector pPUR (Clontech, Mountain View, CA) at a molar ratio of 5:1, followed by selection in the presence of 1 μg/ml puromycin (Sigma-Aldrich, St. Louis, MO). The cells were maintained in Ham's F-12 medium (Wako Pure Chemical Industries, Osaka, Japan) supplemented with 10% fetal bovine serum (FBS; Gibco-Invitrogen, Carlsbad, CA) at 37°C in a humidified incubator containing 5% CO_2 in air. For the experiments, subconfluent cultures were harvested by brief trypsinization (trypsin-EDTA solution; Nacalai Tesque, Kyoto, Japan) and resuspended in Ham's F-12 medium supplemented with 2% FBS. Cell viability was determined by trypan blue staining (Sigma-Aldrich, St. Louis, MO).

Antibiotic preparation. CIP (Wako Pure Chemical Industries, Osaka, Japan) and GRN (kindly provided by Taisho Toyama Pharmaceutical, Tokyo, Japan) were dissolved in dimethyl sulfoxide at a concentration of 30 mg/ml, MFX (Santa Cruz, CA) was dissolved in distilled water at a concentration of 10 mg/ml, and GAT, SPX, and STF (Hokkaido University) were dissolved in 0.1 N NaOH at a concentration of 10 mg/ml.

Determination of OPN protein levels. To measure the OPN levels in the culture supernatants, A549 cells were plated in triplicate at 1×10^4 cells per well in 96-well plates. After 24 h of incubation, the cells were washed twice with serum-free Ham's F-12 medium, and fresh serum-free medium was added. Cells were treated by CIP, GRN, MFX, GAT, SPX, and STF at the indicated concentrations. After further incubation for 48 h, the culture supernatant was harvested and stored at −20°C. The OPN protein levels were measured by a human osteopontin Quantikine enzyme-linked immunosorbent assay (ELISA) kit (R&D Systems, Minneapolis, MN).

Cell viability. To measure the effect of the quinolones on cell viability and proliferation, A549 cells were plated in triplicate at 1×10^4 cells per well in 96-well plates. At 24 and 48 h after the addition of the antibiotics, a 3-(4,5-dimethyl-2-thiazolyl)-2,5-diphenyl-2H-tetrazolium bromide (MTT) assay (Dojindo, Kumamoto, Japan) was performed according to the manufacturer's instructions. Similarly treated wells without cells served as blanks.

Determination of OPN promoter activity. A549/OPN-luc cells were treated the same as for ELISA. For the luciferase assay, at 24 and 48 h after the treatment, cells were washed twice with phosphate-buffered saline (PBS) and then lysed with a luciferase cell culture lysis reagent (Promega, Madison, WI). The luciferase assay was done with a luciferase assay system according to the manufacturer's instructions, and the luciferase activities were measured using a Mithras LB 940 microplate luminometer (Berthold Technologies, Oak Ridge, TN).

AQ: C

qRT-PCR. Quantitative reverse transcription-PCR (qRT-PCR) was performed to examine the effect of quinolones on the expression of OPN mRNA. A549 cells were plated at 1×10^6 in a 6-well plate, and after 24 h, the cells were washed twice with serum-free medium. Fresh serum-free medium and quinolones were added at a final concentration of 30 μg/ml, and GRN was added at a concentration of 1, 3, 10, or 30 μg/ml. The cells were incubated for a further 48 h. Cells were lysed with TRIzol reagent (Invitrogen), and total RNA was extracted according to the manufacturer's instructions. After treatment with RNase-free DNase (Promega), the DNA-free RNA (250 ng) was used for synthesis of the first-strand cDNA at 42°C for 60 min using Moloney murine leukemia virus reverse transcriptase (Invitrogen). Real-time quantitative PCR using Power SYBR green PCR master mix was conducted for 40 cycles at 95°C for 15 s and at 60°C for 1 min in a 96-well format on an ABI StepOne real-time PCR system (Applied Biosystems). Primer sequences were as follows: OPN forward, 5′-ACTCGTCTCAGGCCAGTTG-3′; OPN reverse, 5′-CGTTGGACTTG GAAGG-3′; GAPDH forward, 5′-TGATGACATCAAGAAGGTGG-3′; and GAPDH reverse, 5′-TCCTTGGAGGCCATGTGGGC-3′.

shRNA transfection. To diminish OPN expression, A549 cells were transfected with short hairpin RNA (shRNA) targeting OPN or control shRNA (Santa Cruz Biotechnology, Inc.) with Effectene transfection reagent (Qiagen, Valencia, CA) for 48 h. In another setting, cells were transfected with shRNA targeting OPN for 24 h and then washed twice with serum-free medium. The 24-h-conditioned medium from nontreated cells or cells treated with 30 μl/ml of GRN or SPX was added, and the cells were cultured for a further 24 h. Cells were then analyzed by fluorescence-activated cell sorting (FACS).

Annexin V/7-AAD staining and flow cytometry. A549 cells and cell supernatant were harvested and washed twice with PBS and resuspended in binding buffer containing 10 mM HEPES-NaOH (pH 7.4), 140 mM NaCl, and 2.5 mM $CaCl_2$. A staining mixture consisting of 5 μl annexin V-phycoerythrin and 5 μl 7-aminoactinomycin (7-AAD) (BD Biosciences Pharmingen) was added to 100 μl of cell suspension (1×10^6 cells/ml). Cells were incubated in the dark for 15 min at room temperature and then analyzed on a FACSDiva flow cytometer. Data were analyzed using FlowJo software (FlowJo, Inc.). The cells in early apoptosis were considered to be annexin V positive and 7-AAD negative. Positivity for both annexin V and 7-AAD indicated late apoptosis.

Statistical analysis. Results are expressed as means ± standard errors of the means. The statistical difference was determined by two-sided Student's *t* test, and the correlation between OPN promoter activity and OPN secretion was obtained using simple regression analysis by Statcel2 software (OMS, Tokyo, Japan). A difference with a P value of <0.05 was considered significant.

RESULTS

Quinolones enhance OPN release from A549 alveolar epithelial cells. The A549 cell line, which secretes OPN, serves as a good model to study drug-induced changes in cytokine secretion (13). We found that treatment of the cells with CIP at 30 μg/ml induced a minimal elevation of OPN secretion, while GRN dramatically increased the OPN level in a dose-dependent manner. Treatment with 1 μg/ml to 30 μg/ml of GRN resulted in a 60 to 220% enhancement of OPN secretion. MFX and SPX at doses of 3 μg/ml to 30 μg/ml caused significant OPN enhancements from 23 to 62% and 22 to 79%, respectively. Similarly, 38 to 82% and 23 to 60% elevations of OPN levels were induced by the addition 10 μg/ml to 30 μg/ml of GAT and STF (Fig. 1).

F1

Enhancement of OPN promoter activity. To investigate the

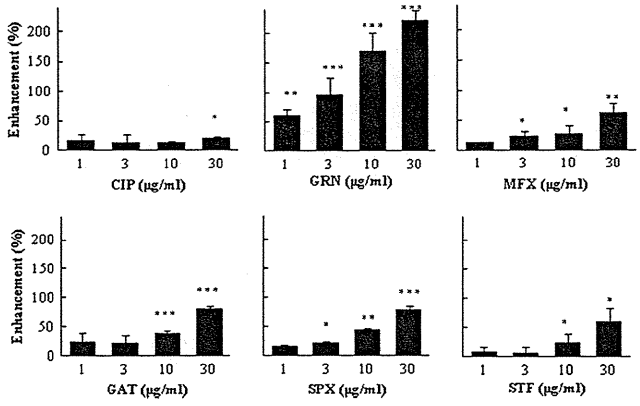

FIG 1 Effect of quinolones on OPN release. A549 cells were plated at 1×10^4 in 96-well plates, and after 24 h, the cells were washed twice with serum-free medium. Fresh serum-free medium and drugs at final concentrations of 1, 3, 10, and 30 μg/ml were added. The cells were incubated for a further 48 h, and the OPN concentrations in the cell culture supernatant were measured by ELISA, as described in Materials and Methods. OPN secretion was normalized by the cell viability optical density (570 to 630 nm) value of the MTT assay and expressed as percent increase above control. Controls are the wells treated only with solvent. The results are expressed as means ± SDs. Representative data of three independent experiments are shown. ***, $P < 0.001$ compared to the control; **, $P < 0.01$ compared to the control; *, $P < 0.05$ compared to the control.

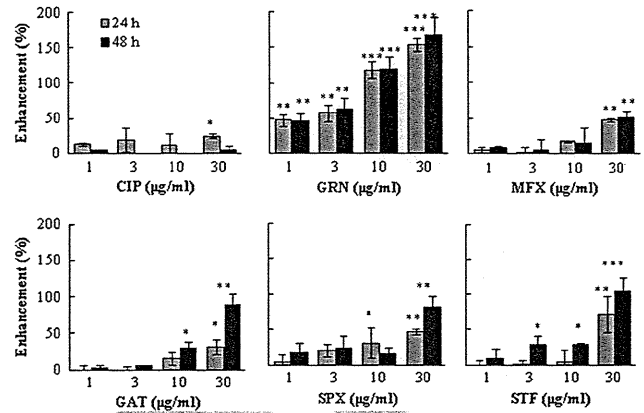

FIG 2 Effect of quinolones on OPN promoter activity. A549 cells were plated at 1×10^4 in 96-well plates, and after 24 h, the cells were washed twice with serum-free medium. Fresh serum-free medium and drugs at final concentrations of 1, 3, 10, and 30 μg/ml were added. Cells were incubated for a further 24 or 48 h, and the OPN gene promoter activity was measured by luciferase assay, as described in Materials and Methods. The OPN promoter activity was normalized by the cell viability optical density (570 to 630 nm) value of the MTT assay and expressed as percent increase above the value for the control. Controls are the wells treated only with solvent. The results are expressed as means ± SDs. Representative data of three independent experiments are shown. ***, $P < 0.001$ compared to the control; **, $P < 0.01$ compared to the control; *, $P < 0.05$ compared to the control.

AQ: E

mechanisms of enhancement the OPN secretion, A549/OPN-luc cells, which stably express OPN promoter/luciferase, were established. Thus, luciferase expression of A549/OPN-luc cells served as a parameter to monitor the level of OPN transcription. CIP at 30 μg/ml induced only a 25% elevation of OPN transcription. In contrast, even 24 h cell exposure to 1 μg/ml to 30 μg/ml of GRN for 24 h induced strong, dose-dependent OPN gene activation, reaching 47 to 160%. A similar finding was observed after 48 h. Enhancement of OPN gene promoter activation was observed with increasing concentrations of MFX, GAT, SPX, and STF. However, the change was not so striking compared to that for GRN (Fig. 2). We also examined the association between OPN promoter activation and OPN secretion and found a statistically significant correlation for GRN and GAT ($P < 0.01$) and for MFX and STF ($P < 0.05$) (Table 1).

F2

T1/AQ:D

Effect of quinolones on OPN mRNA expression. To examine if quinolones alter the expression of OPN mRNA, we performed quantitative reverse transcription-PCR. First, we screened the effects of CIP, GRN, MFX, and SPX at a concentration of 30 μg/ml and found that GRN and MFX significantly enhanced mRNA expression compared to that for the control (Fig. 3A). Next, we analyzed the dose-dependent effect of GRN. When cells were incubated with various concentrations of GRN, we observed the dose-related increase of OPN mRNA expression, with statistical significance achieved at concentrations of 10 and 30 μg/ml (Fig. 3B).

F3

Effect of quinolones on early and late apoptosis. To investigate the effect of quinolones on A549 cell apoptosis, we used annexin V/7-AAD double staining for FACS analysis. Treatment of A549 cells with GRN and SPX at a concentration of 30 μg/ml did not affect early apoptosis, but late apoptosis was decreased by SPX (4.42%) and slightly by GRN (9.25%) compared to the control (12.6%). Downregulation of OPN by shRNA resulted in an increase of both early (6.55%) and late (16.7%) apoptosis. When a 24-h supernatant was added to OPN expression-silenced cells, the percentage of apoptotic cells decreased. Surprisingly, the SPX supernatant prevented late apoptosis (5.13%) (Table 2).

T2

DISCUSSION

In this study, we examined the effect of quinolones on OPN synthesis in A549 human lung epithelial cells. We found that GRN, MFX, GAT, SPX, and STF dose dependently enhanced OPN secretion. On the other hand, CIP at a concentration of 30 μg/ml only slightly enhanced OPN. Since our ELISA system cannot distinguish phosphorylated from nonphosphorylated or cleaved forms of OPN, we could not elucidate which form of OPN was enhanced. To elucidate the mechanism of quinolone-induced OPN elevation, we employed a luciferase assay and found that this elevation occurred at the transcriptional level by activation of the OPN gene promoter. The results of qRT-PCR also revealed that

TABLE 1 Correlation between OPN promoter activity and OPN secretion and maximal serum concentrations of studied quinolones

Drug	Correlation between OPN promoter activity and OPN secretion[a]		Dose (mg)	C_{max}[b] (μg/ml)
	R^2 value	P value		
CIP	0.881	0.061	750 (×2)[c]	3.5
GRN	0.988	0.006**	400 (×1)	5.8
MFX	0.929	0.036*	400 (×1)	3.1
GAT	0.993	0.003**	400 (×1)	4.0
SPX	0.756	0.131	400 (×1)	1.0
STF	0.913	0.045*	200 (×1)	1.9

[a] Luciferase assay and ELISA data from a 48-h quinolone treatment of A549 cells expressing percent increase above the value for the control were assessed by simple regression analysis. **, $P < 0.01$; *, $P < 0.05$.

[b] C_{max}s from previous studies (1, 22).

[c] Data in parentheses represent frequency per day.

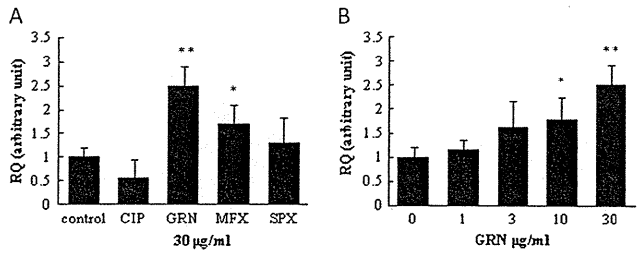

FIG 3 Effect of quinolones on OPN mRNA expression. A549 cells were plated at 1×10^6 in a 6-well plate, and after 24 h, the cells were washed twice with serum-free medium. Fresh serum-free medium and quinolones at a final concentration of 30 μg/ml (A) and GRN at concentrations of 1, 3, 10, and 30 μg/ml (B) were added. The cells were incubated for a further 48 h. Total RNA was isolated, and qRT-PCR was performed as described in Materials and Methods. The results are expressed as means ± SDs. Representative data of three independent experiments are shown. **, $P < 0.01$ compared to the control; *, $P < 0.05$ compared to the control.

MFX and GRN significantly enhanced OPN mRNA expression, but SPX and CIP did not.

Generally, quinolones are thought to attenuate proinflammatory cytokine synthesis, though there have been reports that CIP caused an increase in IL-2 secretion from PMA-treated human peripheral blood lymphocytes. In contrast, there was no effect on IL-1 release in the same experimental setting (33). Because the effect of quinolones on cytokine synthesis is not consistent and differs by the cell type and the cytokine examined (13), it is tempting to speculate that the cytokine response to drug treatment is cell type specific and influenced by the microenvironment under which cells exist.

In our study, we investigated the effect of quinolone concentrations above and below the maximal concentrations in serum (C_{max}s) (Table 1). The results showed that GAT, SPX, and STF augmented OPN transcription only at concentrations higher than the C_{max}s, but GRN and MFX elicited the ability to enhance OPN even at their C_{max}s. Since OPN is a multifunctional protein, an elevation of OPN synthesis might have a dual effect. OPN can promote protective immunity through the OPN-dependent induction of the proinflammatory cytokine IL-12 and suppression of the anti-inflammatory cytokine IL-10 (2). However, the excessive OPN production might activate various cell growth signals, finally leading to oncogenesis (26, 42). Zhang et al. observed that the OPN gene is transactivated up to 5-fold by Tax protein of human T-cell leukemia virus type 1 (42). However, in our study, the therapeutic concentrations of quinolones did not enhance OPN more than 2-fold. Despite our observation of a quinolone-induced OPN enhancement, it is conceivable that such an elevation would not lead to oncogenesis.

Several studies confirmed the antiapoptotic activities of FQs. Azuma et al. suggested that tosufloxacin delayed programmed cell death via the activation of phosphoinositide 3-kinase (PI3K)/Akt and/or p38 MAPK (3). Since OPN is a downstream effector of PI3K/Akt (27, 42) and OPN elicits an antiapoptotic effect (6, 17), we speculate that the antiapoptotic effect of the quinolones is caused by the enhancement of OPN synthesis. We examined the effect of quinolones on early and late stages of apoptosis by FACS analysis. During early apoptosis, the phosphatidylserine (PS) changes location from the cytosolic leaflet to the outer leaflet of the cell. This event can be detected by annexin V, which binds to the PS (16). The damage of the cell membrane during late apoptosis and necrosis allows insertion of 7-AAD between the tops of successive cytosine and guanine bases (41). We could not observe significant changes in early apoptosis upon quinolone treatment, but SPX considerably decreased late apoptosis in A549 cells. We found that the cell culture medium from SPX-treated cells prevented late apoptosis in OPN shRNA-transfected A549 cells, but GRN-treated and untreated cell supernatants had only minor effects. Among the studied quinolones, GRN exerted the greatest ability to enhance OPN synthesis and did not significantly alter early or late apoptosis in A549 cells. OPN synthesis was also enhanced by SPX treatment but to a lesser extent than by GRN, but an effect of SPX on late apoptosis was clearly observed. This made us conclude that there might be other factors which prevent apoptosis upon quinolone treatment and that the OPN might have only a supportive effect or the OPN enhancement was not sufficient to exert its antiapoptotic property.

Throughout respiratory infections, apoptosis may be beneficial or detrimental for the host (4). In infections in which pathogens exist within the host cells, apoptosis favors the host. Insufficient apoptosis of alveolar macrophages during tuberculosis infection leads to the chronicity and dissemination of the infection. For extracellular infections, apoptosis of the immune inflammatory cells potentiates the viability of the pathogen and promotes the infection (4). Our *in vitro* finding showed that SPX decreased late apoptosis in A549 cells. The antiapoptotic effect of quinolones on lung epithelial cells *in vivo* remains to be elucidated.

The quinolones used in our study differ in chemical structure as well as in the ability to influence OPN secretion and apoptosis. The fluorine molecule at the C-6 position, which is present in CIP, MFX, GAT, SPX, STF, and other FQs, is thought to improve the antimicrobial properties of these drugs, but the newly developed GRN is lacking this moiety. GRN has fluorine incorporated through a C-8 difluoromethyl ester linkage (1). Manipulation of the group at position C-8 has also been shown to play a role in broadening the spectrum of activity (12). Among the studied

TABLE 2 FACS analysis showing early and late apoptosis

Treatment[a]	% cells showing[b]: Early apoptosis	Late apoptosis
Control	3.28	12.6
DMSO (5%)	10.9	33.8
GRN	4.82	9.25
SPX	4.74	4.42
shRNA	6.55	16.7
Negative-control shRNA	5.33	13.6
shRNA + control supernatant	4.61	12.2
shRNA + GRN supernatant	4.99	14.3
shRNA + SPX supernatant	4.98	5.13

[a] A549 cells were plated at 1×10^6 cells per well in 6-well plates. After 24 h of incubation, the cells were washed twice with serum-free Ham's F-12 medium and fresh serum-free medium containing 5% DMSO as a positive control or GRN and SPX at a final concentration of 30 μl/ml, or cells were transfected with shRNA against OPN or negative-control shRNA. Cells were then incubated for a further 48 h and analyzed. Other cells were transfected with shRNA against OPN for 24 h. After the medium was removed, cells were washed twice with serum-free medium; 24-h-conditioned medium from untreated (control supernatant), GRN-treated (30 μg/ml), or SPX-treated (30 μg/ml) cells was added; and cells were incubated for a further 24 h. FACS analysis was performed as described in Materials and Methods. Representative data of three independent experiments are shown.

[b] Cells showing early apoptosis are annexin positive and 7-AAD negative. Cells showing late apoptosis are annexin V positive and 7-AAD positive.

quinolones, only CIP is lacking the substituent at C-8. Our results showed that in contrast to CIP, GRN significantly enhanced OPN production. Therefore, we speculate that the ability of quinolones to enhance OPN production may be associated with the presence of the C-8 substituent.

In conclusion, we found that quinolones enhance OPN synthesis by activation of the OPN gene promoter. The antiapoptotic effects of quinolones do not appear to be associated with OPN elevation. Our study supports the idea that quinolones have immunomodulatory properties.

ACKNOWLEDGMENTS

This work is supported by the Scientific Research Expenses for Health and Welfare program from the Ministry of Health, Labor and Welfare, Japan (to T.H.), and the Science and Technology Research Partnership for Sustainable Development from the Japan Science and Technology Agency, Japan (to Y.S.). This work was supported by collaborative funding from the Research Centre for Zoonosis Control, Hokkaido University.

We are grateful to Shenwei Li, Xiaoguang Li, and Yuko Sato (Tohoku University) for technical assistance. We thank Brent Bell for reading the manuscript.

We declare no competing financial interest.

AQ: ref

REFERENCES

1. Andersson MI, MacGowan AP. 2003. Development of the quinolones. J. Antimicrob. Chemother. 51(Suppl. 1):1–11.
2. Ashkar S, et al. 2000. Eta-1 (osteopontin): an early component of type-1 (cell-mediated) immunity. Science 287:860–864.
3. Azuma Y, Ohura K. 2003. Alteration of constitutive apoptosis in neutrophils by quinolones. Inflammation 27:115–122.
4. Behnia M, Robertson KA, Martin WJ II. 2000. Lung infections: role of apoptosis in host defense and pathogenesis of disease. Chest 117:1771–1777.
5. Brown LF, et al. 1992. Expression and distribution of osteopontin in human tissues: widespread association with luminal epithelial surfaces. Mol. Biol. Cell 3:1169–1180.
6. Burdo TH, Wood MR, Fox HS. 2007. Osteopontin prevents monocyte recirculation and apoptosis. J. Leukoc. Biol. 81:1504–1511.
7. Cantor H, Shinohara ML. 2009. Regulation of T-helper-cell lineage development by osteopontin: the inside story. Nat. Rev. Immunol. 9:137–141.
8. Christensen B, et al. 2007. Cell type-specific post-translational modifications of mouse osteopontin are associated with different adhesive properties. J. Biol. Chem. 282:19463–19472.
9. Christensen B, Nielsen MS, Haselmann KF, Petersen TE, Sorensen ES. 2005. Post-translationally modified residues of native human osteopontin are located in clusters: identification of 36 phosphorylation and five O-glycosylation sites and their biological implications. Biochem. J. 390:285–292.
10. Dalhoff A. 2005. Immunomodulatory activities of fluoroquinolones. Infection 33(Suppl. 2):55–70.
11. Diamond G, Legarda D, Ryan LK. 2000. The innate immune response of the respiratory epithelium. Immunol. Rev. 173:27–38.
12. Dong Y, Xu C, Zhao X, Domagala J, Drlica K. 1998. Fluoroquinolone action against mycobacteria: effects of C-8 substituents on growth, survival, and resistance. Antimicrob. Agents Chemother. 42:2978–2984.
13. Donnarumma G, et al. 2007. Anti-inflammatory effects of moxifloxacin and human beta-defensin 2 association in human lung epithelial cell line (A549) stimulated with lipopolysaccharide. Peptides 28:2286–2292.
14. Drlica K, Zhao X. 1997. DNA gyrase, topoisomerase IV, and the 4-quinolones. Microbiol. Mol. Biol. Rev. 61:377–392.
15. Gogos CA, et al. 2004. Comparative effects of ciprofloxacin and ceftazidime on cytokine production in patients with severe sepsis caused by gram-negative bacteria. Antimicrob. Agents Chemother. 48:2793–2798.
16. Koopman G, et al. 1994. Annexin V for flow cytometric detection of phosphatidylserine expression on B cells undergoing apoptosis. Blood 84:1415–1420.
17. Lin YH, Yang-Yen HF. 2001. The osteopontin-CD44 survival signal involves activation of the phosphatidylinositol 3-kinase/Akt signaling pathway. J. Biol. Chem. 276:46024–46030.
18. MacRedmond R, Greene C, Taggart CC, McElvaney N, O'Neill S. 2005. Respiratory epithelial cells require Toll-like receptor 4 for induction of human beta-defensin 2 by lipopolysaccharide. Respir. Res. 6:116.
19. Maeno Y, et al. 2006. Osteopontin participates in Th1-mediated host resistance against nonlethal malaria parasite Plasmodium chabaudi chabaudi infection in mice. Infect. Immun. 74:2423–2427.
20. Moadebi S, Harder CK, Fitzgerald MJ, Elwood KR, Marra F. 2007. Fluoroquinolones for the treatment of pulmonary tuberculosis. Drugs 67:2077–2099.
21. Morimoto Y, et al. 2011. Osteopontin modulates the generation of memory CD8+ T cells during influenza virus infection. J. Immunol. 187:5671–5683.
22. Nakashima M, et al. 1995. Pharmacokinetics and tolerance of DU-6859a, a new fluoroquinolone, after single and multiple oral doses in healthy volunteers. Antimicrob. Agents Chemother. 39:170–174.
23. Nau GJ, et al. 2000. Osteopontin expression correlates with clinical outcome in patients with mycobacterial infection. Am. J. Pathol. 157:37–42.
24. Nau GJ, et al. 1999. Attenuated host resistance against Mycobacterium bovis BCG infection in mice lacking osteopontin. Infect. Immun. 67:4223–4230.
25. Niwa M, et al. 2004. P38 MAPK associated with stereoselective priming by grepafloxacin on O-2(−) production in neutrophils. Free Radic. Biol. Med. 36:1259–1269.
26. O'Regan A. 2003. The role of osteopontin in lung disease, Cytokine Growth Factor Rev. 14:479–488.
27. Packer L, et al. 2006. Osteopontin is a downstream effector of the PI3-kinase pathway in melanomas that is inversely correlated with functional PTEN. Carcinogenesis 27:1778–1786.
28. Rollo EE, et al. 2005. The cytokine osteopontin modulates the severity of rotavirus diarrhea. J. Virol. 79:3509–3516.
29. Shinohara ML, Kim HJ, Kim JH, Garcia VA, Cantor H. 2008. Alternative translation of osteopontin generates intracellular and secreted isoforms that mediate distinct biological activities in dendritic cells. Proc. Natl. Acad. Sci. U. S. A. 105:7235–7239.
30. Shinohara ML, et al. 2006. Osteopontin expression is essential for interferon-alpha production by plasmacytoid dendritic cells. Nat. Immunol. 7:498–506.
31. Sodek J, Ganss B, McKee MD. 2000. Osteopontin. Crit. Rev. Oral Biol. Med. 11:279–303.
32. Sorensen ES, Hojrup P, Petersen TE. 1995. Posttranslational modifications of bovine osteopontin: identification of twenty-eight phosphorylation and three O-glycosylation sites. Protein Sci. 4:2040–2049.
33. Stunkel KG, Hewlett G, Zeiler HJ. 1991. Ciprofloxacin enhances T cell function by modulating interleukin activities. Clin. Exp. Immunol. 86:525–531.
34. Takeyama K, et al. 2007. The 6-fluoro-8-methoxy quinolone gatifloxacin down-regulates interleukin-8 production in prostate cell line PC-3. Antimicrob. Agents Chemother. 51:162–168.
35. Tsivkovskii R, et al. 2011. Levofloxacin reduces inflammatory cytokine levels in human bronchial epithelia cells: implications for aerosol MP-376 (levofloxacin solution for inhalation) treatment of chronic pulmonary infections. FEMS Immunol. Med. Microbiol. 61:141–146.
36. Uede T. 2011. Osteopontin, intrinsic tissue regulator of intractable inflammatory diseases. Pathol. Int. 61:265–280.
37. Uede T, Katagiri Y, Iizuka J, Murakami M. 1997. Osteopontin, a coordinator of host defense system: a cytokine or an extracellular adhesive protein? Microbiol. Immunol. 41:641–648.
38. Weiss T, et al. 2004. Anti-inflammatory effects of moxifloxacin on activated human monocytic cells: inhibition of NF-kappaB and mitogen-activated protein kinase activation and of synthesis of proinflammatory cytokines. Antimicrob. Agents Chemother. 48:1974–1982.
39. Werber S, et al. 2005. Moxifloxacin inhibits cytokine-induced MAP kinase and NF-kappaB activation as well as nitric oxide synthesis in a human respiratory epithelial cell line. J. Antimicrob. Chemother. 55:293–300.
40. Yasumoto R, et al. 1995. Seminal plasma cytokines in nonbacterial prostatitis: changes following sparfloxacin treatment. Hinyokika Kiyo 41:771–774.
41. Zelenin AV, et al. 1984. 7-Amino-actinomycin D as a specific fluorophore for DNA content analysis by laser flow cytometry. Cytometry 5:348–354.
42. Zhang J, Yamada O, Matsushita Y, Chagan-Yasutan H, Hattori T. 2010. Transactivation of human osteopontin promoter by human T-cell leukemia virus type 1-encoded Tax protein. Leuk. Res. 34:763–768.

pagepress

Rapid detection of *Mycobacterium tuberculosis* complex in cattle and lechwe (*Kobus leche kafuensis*) at the slaughter house

Mudenda B. Hang'ombe,[1] Chie Nakajima,[2] Akihiro Ishii,[2] Yukari Fukushima,[2] Musso Munyeme,[1] Wigganson Matandiko,[3] Aaron S. Mweene,[1] Yasuhiko Suzuki[2,4]

[1]School of Veterinary Medicine, University of Zambia, Lusaka, Zambia; [2]Hokkaido University Research Center for Zoonosis Control, Sapporo, Hokkaido, Japan; [3]Zambia Wildlife Authority, Private Bag 001, Chilanga, Zambia; [4]JST/JICA-SATREPS

Abstract

The detection and diagnosis of tuberculosis (TB) in food-producing animals is critical to human health. In this study we applied the loop-mediated isothermal amplification (LAMP) system to detect *Mycobacterium tuberculosis* complex (MTC) directly in 57 cattle and six lechwe (*Kobus leche kafuensis*) carcasses exhibiting lesions characteristic of TB. The samples were first subjected to Ziehl-Neelsen microscopy, followed by culture and LAMP assay. In addition, multiplex-PCR was used to determine the species involved. Of the samples from the cattle, 84.2% (95% confidence interval: 71.6-92.1) were found positive with Ziehl-Neelsen microscopy, 93.0% (95% confidence interval: 82.2-97.7) with culture, and 94.7% (95% confidence interval: 84.5-98.6) with the LAMP system while the *Kobus leche kafuensis* samples were all positive for all techniques used. These results indicate that the LAMP system can be used to augment the detection and surveillance of TB in animals; hence can be a very useful tool in the veterinary field and in public health.

Introduction

The detection and diagnosis of tuberculosis (TB) in animals involves clinical examination, tuberculin skin tests, and the gamma interferon immunoassay.[1,2] Other techniques involve detection on meat inspection or postmortem followed by the usual course of microscopic observation of acid-fast bacilli, bacterial cultures, and molecular confirmation methods.[3] TB in animals can be caused by *Mycobacterial* species belonging to the *Mycobacterium tuberculosis* complex (MTC). This group comprises several closely related species responsible for strictly human and zoonotic TB. These include *M. tuberculosis, M. africanum, M. microti, M. bovis, M. caprae*, and *M. pinnipedii*.[4-6] Some of these *Mycobacterium* species are major re-emerging zoonotic agents of bovine TB, the prevalence of which depends on direct exposure to cattle and consumption of unpasteurized dairy products.[7,8] Furthermore, the interaction in the human-livestock-wildlife interphase areas of some wildlife animals like lechwe (*Kobus leche kafuensis*), documented with *M. bovis*, have broadened the reservoir base for MTC.[9]

In this regard, detection and diagnosis of TB is very important as a way of mitigating its spread in the human population. Currently, a novel molecular amplification method termed the loop-mediated isothermal amplification system (LAMP) has been developed.[10] The system shows a high amplification efficiency and has been used to diagnose several other diseases.[10-17] The objective of our study was to evaluate the applicability of the LAMP system, in the veterinary field, to detect MTC directly from suspected TB lesions of cattle and wildlife being slaughtered for food.

Materials and Methods

Sampling

Our study was conducted on samples collected from the slaughtered animals along the examination line. The animals were examined for gross lesions according to the standard postmortem procedures as described previously.[18] Organs and tissues with suspected TB lesions were collected after detailed postmortem examination of the entire carcasses. Following collection, the specimens were placed into a cooler box with ice packs before transportation to the laboratory for analysis.

Preparation of samples for evaluation

To prepare the suspected TB samples for analysis, the suspected tissues with lesions were trimmed of fat and then a 500-mg sample was collected. The sample was then minced with sterile scissors and homogenized in a sterilized glass homogenizer, after which 1 mL of phosphate buffer (pH 6.8) was added. After thorough mixing, 1 mL of 5% sodium hydroxide was added. This was mixed thoroughly and then incubated for 15 min at room temperature. To this mixture 10 mL of phosphate buffer was added and then centrifuged at 1500 *g* for 20 min. The pellet was collected and then resuspended in a final volume of 0.5 mL of phosphate buffer. This was used for inoculation into 2% Ogawa medium and preparation of slides for Ziehl-Neelsen (ZN) microscopy. Cultures were monitored for growth up to 8 wk at 37°C. Another 100 μL of the suspension was used to prepare DNA directly by using DNAzol reagent (Invitrogen, Carlsbad, CA, USA). The suspension was mixed with 1.0 mL of DNAzol reagent and mechanical disruption was used as previously described.[19] DNA was extracted according to the manufacturer's instructions. Genomic DNA from *Mycobacterium* bacterial cultures was also prepared from colonies using DNAzol and mechanical disruption as described earlier. The extracted DNA was then dissolved in 50 μL TE buffer consisting of 10 mM Tris/HCL (pH 8.0) and 1 mM EDTA.

Correspondence: Mudenda Bernard Hang'ombe, School of Veterinary Medicine, Department of Paraclinical Studies, P. O. Box 32379, Lusaka, Zambia.
E-mail: mudenda68@yahoo.com

Key words: *Mycobacterium bovis*, cattle, *Kobus leche kafuensis*, LAMP, multiplex-PCR.

Acknowledgments: the authors are grateful to Mr L. Moonga and Mr E. Mulenga from the Department of Paraclinical Studies, School of Veterinary Medicine, University of Zambia for their technical assistance. This work was supported by the Directorate of Research and Graduate Studies of the University of Zambia, the Ministry of Education, Culture, Sports, Science and Technology of Japan (MEXT), and the Global Center of Excellence (COE) program for the Establishment of International Collaboration Centers for Zoonoses control, by grants from the US-Japan Cooperative Medical Science program to YS and the Japan Society for the Promotion of Science to YS and CH.

Contributions: MBH, sample collection, isolation, LAMP and PCR detection, analysis, data interpretation, and manuscript drafting; CN, AI, YF, MM, WM, design of study, sample collection, and manuscript drafting; ASM, YS, interpretation of data, drafting, and final approval of manuscript.

Conflict of interest: the authors report no conflicts of interest.

Received for publication: 3 March 2011.
Accepted for publication: 29 April 2011.

Veterinary Science Development 2011; 1:e5
doi:10.4081/vsd.2011.e5

LAMP

LAMP reactions were performed in a total volume of 25 μL consisting of 30 pmol each of inner primers FIP and BIP, 5 pmol each of outer primers F3 and B3, 20 pmol each of loop primers FLP and BLP, 1.4 mM deoxynucleotide triphosphate, 0.8 M betaine, 20 mM Tris/HCl (pH 8.8), 10 mM KCl, 10 Mm $(NH4)_2SO_4$, 8 mM $MgSO_4$ and 8 U Bst DNA polymerase (New England Biolabs, USA) with 2 μL sample DNA. The sequences of the primers used are shown in Table 1.

The primers used in our study have also been used by other workers to detect MTC in human sputum samples.[17] The mixture was then incubated at 64°C for 1 hr in a thermal dry heat block (ALB 221; Iwaki, Tokyo, Japan). A negative control (buffer) and positive control were included in each run. Results were visualized with the fluorescence detection reagent (Eiken Chemical Co., Tochigi, Japan) according to the manufacturer's instructions.

Multiplex-PCR primers and conditions

Genomic DNA from *Mycobacterium* bacterial cultures was used as a template. Primer pairs for *cfp32* (a specific gene for MTC), RD9 (region of difference 9 seen only in *M. tuberculosis* and *M. canettii*), and RD12 (region of difference 12 deleted in *M. bovis, M. caprae*, and *M. canettii*) were obtained from an earlier publication.[20] The general PCR recipe contained 7.4 μL H_2O, 2 μL 10 x Taq buffer, 2 μL dNTPs (2.5 mM each), 0.2 μL Taq (Takara), 1 μL target DNA, 2.2 μL of 10 μM *cfp32* primers, 0.7 μL of 5 μM RD9 primers, and 0.8 μL of 5 μM RD12 primers. Appropriate negative controls consisting of PCR mix without target DNA were included. The PCR was performed using the following program: denaturation for 1 min at 98°C followed by 35 cycles of 5 sec at 98°C, 20 sec at 58°C, and 1 min at 68°C with final extension for 5 min at 72°C in a thermalcycler (iCycler, Bio-Rad Laboratories Inc., CA, USA). All PCR products were identified by gel electrophoresis in a 2.0% agarose gel and were visualized by ethidium bromide staining.

Results

A total of 388 carcasses were examined, comprising 358 cattle and 30 lechwe. Of these animals examined, 57 (15.9% CI: 12.4-20.2) cattle carcasses had lesions characteristic of TB in the tissues and organs while 6 (20% CI: 8.40-39.1) lechwe carcasses had such lesion exhibitions as well. When these samples were subjected to ZN microscopy, 48 (84.2% CI: 71.6-92.1) and 6 (100% CI: 51.7-100) samples from the cattle and lechwe, respectively, were found positive. In the case of the cattle, 9 samples were found to be negative, from those observed with characteristic TB lesions. On culture of postmortem TB-positive samples, 53 (93.0% CI: 82.2-97.7) cattle and all lechwe observed at meat inspection were found to be positive for acid-fast bacilli. The positive sample specimens increased in number with the LAMP system. Furthermore, the positive reactions on LAMP were easy to determine with the naked eye, as shown in Figure 1.

Table 1. Primers for the specific detection of the *Mycobacterium tuberculosis* complex used in the study.

Name of primer	Sequence
FIP	CACCCACGTGTTACTCATGCAAGTCGAACGGAAAGGTCT
BIP	TCGGGATAAGCCTGGACCACAAGACATGCATCCCGT
F3	CTGGCTCAGGACGAACG
B3	GCTCATCCCACACCGC
FLP	GTTCGCCACTCGAGTATCTCCG
BLP	GAAACTGGGTCTAATACCGG

Table 2. Number and percentage of samples testing positive for *Mycobacterium tuberculosis* under different procedures.

Sample source	Ziehl-Neelsen microscopy	Culture	LAMP
Cattle	48 (84.2%)	53 (93.0%)	54 (94.7%)
Lechwe	6 (100%)	6 (100%)	6 (100%)
Total	54	59	60
Sensitivity	85.7%	93.7%	95.2%
95% CI	74.1-92.9	83.7-97.9	85.8-98.8

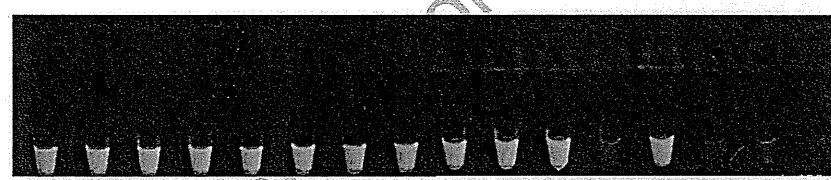

Figure 1. Visual detection of LAMP products under the UV light. From left to right, tubes12, 14, 15, and 16 are negative, while the rest are positive.

The overall results for the detection of TB-positive samples are shown in Table 2. All of the culture positive samples were positive on the LAMP assay. The culture isolates were also subjected to the LAMP system and were found to be MTC. In terms of sensitivity, the LAMP system was 100% positive in culture positive specimens. An additional sample not detected with culture was also found to be positive. The sensitivity of ZN microscopy was found to be 85.7%, while culture was 93.7%, and LAMP 95.2%, respectively. In all these diagnostic procedures, sensitivity was taken as the proportion of samples testing positive for *Mycobacterium* tuberculosis.

The multiplex-PCR was successfully used to identify the MTC species involved in cattle and lechwe. The amplicon of 786bp of the *cfp32* region was observed as indicated in Figure 2,

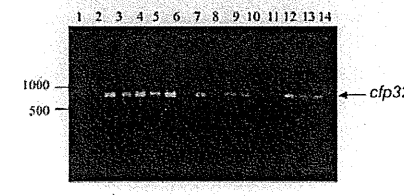

Figure 2. Multiplex-PCR products analyzed with 2% agarose gel electrophoresis followed by ethidium bromide staining. Lane 1 is a 50 bp ladder and lane 13 is a negative control.

showing that the MTC species involved in these cases was *M. bovis*. All of the cultures were positive for this amplicon indicating the MTC strain in the domestic and wildlife animals to be *M. bovis*.

Discussion

We successfully applied the LAMP assay technique for the rapid detection of the MTC group directly from clinical samples. It is important to note that the diagnosis of TB in

animals largely depends on the tuberculin skin testing and slaughterhouse surveillance for undetected infections.[1] In addition, it would be useful to develop a rapid and sensitive method to apply to doubtful TB-suspected samples. Slaughterhouse surveillance of TB is one of the key tools for detecting and confirming suspected TB cases. This is aided by microscopic analysis of sample smears, which is a rapid method of detecting acid-fast bacilli.[3] However, this method is limited in sensitivity and the ability to identify infecting species. The culture method can be used efficiently to diagnose TB, but it is time consuming as it requires a minimum of four weeks. Therefore, a test that combines the rapidity of microscopy and sensitivity of bacterial culture methods would facilitate easy diagnosis at slaughter houses and establishments requiring definite results at the shortest possible time. The test can be a valuable tool in veterinary diagnostics. In our study, there was efficient amplification of the LAMP system to detect MTC from suspected specimens from cattle and lechwe. These results clearly demonstrate the high sensitivity of the LAMP system in detecting TB as observed by others who have been working on human specimens.[11,17,21] This result also suggests that LAMP may be superior to all procedures being used at the moment to detect TB in animals. One sample was detected as positive on LAMP although negative on culture. This could be attributed to low numbers of MTC viable cells in the section of the specimen under investigation. *M. bovis* was identified from the results of the multiplex-PCR, which targets three genetic regions that are *cfp32*, RD9 and RD12.[6,22-24]

In summary, our study clearly provides evidence that the LAMP assay is a method that allows direct detection of MTC from processed clinical/abattoir specimens. This means that the technique can also be applied in the field of veterinary medicine for rapid confirmation of suspected cases. The ease of use and high sensitivity of this assay may facilitate the diagnosis and confirmation of MTC at slaughter houses, hence improving surveillance and control of TB at herd levels and in veterinary medicine in general.

References

1. de la Rua-Domenech R, Goodchild AT, Vordermeier HM, et al. Ante mortem diagnosis of tuberculosis in cattle: a review of the tuberculin tests, gamma-interferon assay and other ancillary diagnostic techniques. Res Vet Sci 2006;81:190-210.
2. Schiller I, Vordermeier HM, Waters WR, et al. Comparison of tuberculin activity using the interferon-gamma assay for the diagnosis of bovine tuberculosis. Vet Rec 2010:167:322-36.
3. Kent BD, Kubica GP. Public Health Mycobacteriology: a Guide for the Level III Laboratory. Atlanta: U.S. Department of Health and Human services, Centers for Disease Control, 1985.
4. Aranaz A, Cousins D, Mateos A, Dominquez, L. Elevation of Mycobacterium tuberculosis subsp. caprae Aranaz et al. 1999 to species rank as Mycobacterium caprae comb. Nov., sp. Nov. Int J Syst Evol Micr 2003;53:1785-9.
5. Cousins DV, Bastida R, Cataldi A, et al. Tuberculosis in seals caused by a novel member of the Mycobacterium tuberculosis complex: Mycobacterium pinnipedii sp. Nov. Int J Syst Evol Micr 2003;53:1305-14.
6. Huard RC, Fabre M, Haas PD, et al. Novel genetic polymorphisms that further delineate the phylogeny of the Mycobacterium tuberculosis complex. J Bacteriol 2006;188:4271-87.
7. Cosivi O, Grange JM, Daborn CJ, et al. Zoonotic tuberculosis due to Mycobacterium bovis in developing countries. Emerg Infect Dis 1998;4:59-70.
8. Michel AL. Implications of tuberculosis in African wildlife and livestock. Ann NY Acad Sci 2002;969:251-5.
9. Pandey GS. Studies of the infectious diseases of the Kafue lechwe (Kobus lechwe kafuensis) with particular reference to tuberculosis in Zambia. PhD thesis, Azabu, University, Tokyo, Japan, 1998.
10. Notomi T, Okayama H, Masubuchi H, et al. Loop-mediated isothermal amplification of DNA. Nucleic Acids Res 2000;28:E63.
11. Iwamoto T, Sonobe T, Hayashi K. Loop-mediated isothermal amplification for direct detection of Mycobacterium tuberculosis complex, M. avium and M. intracellulare. J Clin Microbiol 2003;41:2616-22.
12. Kuboki N, Inoue N, Sakurai T, et al. Loop-mediated isothermal amplification for detection of African trypanosomes. J Clin Microbiol 2003;41:5517-24.
13. Parida M, Posadas G, Inoue GPS, Hasebe F, Morita K. Real-time reverse transcription loop-mediated isothermal amplification for rapid detection of West Nile virus. J Clin Microbiol 2004;42:257-63.
14. Parida M, Horioke K, Ishida H, et al. Rapid detection and differentiation of dengue virus serotypes by a real-time reverse transcription-loop mediated isothermal amplification assay. J Clin Microbiol 2005;43:2895-903.
15. Kimura H, Ihara M, Enomoto Y, et al. Rapid detection of herpes simplex virus DNA in cerebrospinal fluid: comparison between loop-mediated isothermal amplification and real-time PCR. Med Microbiol Immun 2005;194:181-5.
16. Yoda T, Suzuki Y, Yamazaki K, et al. Evaluation and application of reverse transcription loop-mediated isothermal amplification for detection of noroviruses. J Med Virol 2007;79:326-34.
17. Pandey BD, Poudel A, Yoda T, et al. Development of an in-house loop-mediated isothermal amplification (LAMP) assay for detection of Mycobacterium tuberculosis and evaluation in sputum samples of Nepalese patients. J Med Microbiol 2008;57:439-43.
18. Gracey JF, Collins DS, Huey J. eds. Meat Hygiene. 10th edn. Toronto: WB Saunders & Company, 1999.
19. Suzuki Y, Katsukawa C, Inoue K, et al. Mutations in rpoB gene of rifampicin resistant clinical isolates of Mycobacterium tuberculosis in Japan. Kansenshogaku Zasshi 1995;69:413-19.
20. Nakajima C, Rahim Z, Fukushima Y, et al. Identification of Mycobacterium tuberculosis clinical isolates in Bangladesh by a species distinguishable multiplex PCR. BMC Infect Dis 2010;10:118.
21. Boehme CC, Nabeta P, Henostroza G, et al. Operational feasibility of using loop mediated isothermal amplification for diagnosis of pulmonary tuberculosis in microscopy centers of developing countries. J Clin Microbiol 2007;45:1936-40.
22. Brosch R, Gordon SV, Marmiesse M, et al. A new evolutionary scenario for the Mycobacterium tuberculosis complex. Proc Natl Acad Sci USA 2002;99:3684-9.
23. Huard RC, Lazzarini LC, Butler WR, Van Soolingen D, Ho JL. PCR based method to differentiate the subspecies of the Mycobacterium tuberculosis Complex on the basis of genomic deletions. J Clin Microbiol 2003;41:1637-50.
24. Huard RC, Chitale S, Leung M, et al. The Mycobacterium tuberculosis complex restricted gene cfp32 encodes an expressed protein that is detectable in tuberculosis patients and is positively correlated with pulmonary interleukin-10. Infect Immun 2003;71:6871-83.

ANTIMICROBIAL AGENTS AND CHEMOTHERAPY, Aug. 2011, p. 3661–3667 Vol. 55, No. 8
0066-4804/11/$12.00 doi:10.1128/AAC.00042-11

Impact of the E540V Amino Acid Substitution in GyrB of *Mycobacterium tuberculosis* on Quinolone Resistance▽†

Hyun Kim,[1] Chie Nakajima,[1] Kazumasa Yokoyama,[1] Zeaur Rahim,[2] Youn Uck Kim,[3] Hiroki Oguri,[4] and Yasuhiko Suzuki[1,5]*

Department of Global Epidemiology, Hokkaido University Research Center for Zoonosis Control, Sapporo 001-0020, Japan[1]; Tuberculosis Laboratory, International Center for Diarrheal Disease Research, Bangladesh, Dhaka 1000, Bangladesh[2]; Department of Biomedical Sciences, Sun Moon University, A-San 336-708, Republic of Korea[3]; Division of Chemistry, Graduate School of Science, and Division of Innovative Research, Creative Research Institution (CRIS), Hokkaido University, North 21, West 10, Kita-ku, Sapporo 001-0021, Japan[4]; and JST/JICA-SATREPS, Tokyo 120-8666, Japan[5]

Received 11 January 2011/Returned for modification 8 February 2011/Accepted 20 May 2011

Amino acid substitutions conferring resistance to quinolones in *Mycobacterium tuberculosis* have generally been found within the quinolone resistance-determining regions (QRDRs) in the A subunit of DNA gyrase (GyrA) rather than the B subunit of DNA gyrase (GyrB). To clarify the contribution of an amino acid substitution, E540V, in GyrB to quinolone resistance in *M. tuberculosis*, we expressed recombinant DNA gyrases in *Escherichia coli* and characterized them *in vitro*. Wild-type and GyrB-E540V DNA gyrases were reconstituted *in vitro* by mixing recombinant GyrA and GyrB. Correlation between the amino acid substitution and quinolone resistance was assessed by the ATP-dependent DNA supercoiling assay, quinolone-inhibited supercoiling assay, and DNA cleavage assay. The 50% inhibitory concentrations of eight quinolones against DNA gyrases bearing the E540V amino acid substitution in GyrB were 2.5- to 36-fold higher than those against the wild-type enzyme. Similarly, the 25% maximum DNA cleavage concentrations were 1.5- to 14-fold higher for the E540V gyrase than for the wild-type enzyme. We further demonstrated that the E540V amino acid substitution influenced the interaction between DNA gyrase and the substituent(s) at R-7, R-8, or both in quinolone structures. This is the first detailed study of the contribution of the E540V amino acid substitution in GyrB to quinolone resistance in *M. tuberculosis*.

A major human infectious disease, tuberculosis (TB) is estimated to affect approximately one-third of the world's population, and 95% of cases occur in developing countries (15, 30, 31). Current estimates show that approximately 9.4 million new cases and nearly 1.7 million deaths from TB occur each year, and TB remains a major cause of premature death (36).

The increased incidence of multidrug-resistant (MDR) TB (TB resistant to more than two anti-TB drugs, including rifampin and isoniazid [35]) has hampered the treatment and control of TB and is associated with an increase in mortality rates in people with TB (3, 37, 40). Consequently, the required drug dosage for the treatment of TB has dramatically increased (38), and fluoroquinolones (FQs) are now considered to be important second-line anti-TB agents (13, 20).

FQs are a large and widely used class of synthetic antibacterial agents (10, 11, 21, 39) which are frequently used in treating patients infected with MDR TB (6, 17, 22). The target of the FQs in *Mycobacterium tuberculosis* is DNA gyrase, which consists of two subunits, GyrA and GyrB, that form the catalytically active $GyrA_2GyrB_2$ heterotetrameric structure (7, 9, 18). DNA gyrase is an ATP-dependent enzyme that transiently cleaves and unwinds double-stranded DNA (9) to catalyze the negative supercoiling of DNA and is thus essential for efficient DNA replication, transcription, and recombination (7, 24, 29). Most eubacteria, such as *Escherichia coli*, have two DNA topoisomerases, DNA gyrase and topoisomerase IV. A few bacteria, however, such as *M. tuberculosis*, have only DNA gyrase (8), which is therefore the sole target of quinolones.

The quinolone-binding sites in DNA gyrase have been found to be in the quinolone resistance-determining regions (QRDRs) in the GyrA subunit (amino acids Gly-88 to Asp-94 in *M. tuberculosis*) and the GyrB subunit (amino acids Asp-500 to Asn-538 in *M. tuberculosis*), which contain the majority of the amino acid substitutions that confer quinolone resistance (Fig. 1) (2, 19, 27, 32, 33). A recent study using three-dimensional structure analysis, however, has suggested that QRDRs of *M. tuberculosis* gyrase are located at amino acids Ser-73 to Gln-113 of the GyrA subunit and Asn-493 to Asn-540 of the GyrB subunit (28). The QRDRs in GyrB are thought to interact with those in GyrA and DNA strands to form a quinolone-binding pocket (QBP).

In this study, we elucidated the contribution of an amino acid substitution located at position 540 that is found in a quinolone-resistant clinical isolate by *in vitro* DNA supercoiling and cleavage assays in the presence or absence of FQs. We also propose the mechanism of interaction between substituents of FQs and amino acid residues in the QBP of GyrB.

MATERIALS AND METHODS

Reagents and kits. Gatifloxacin (GAT), levofloxacin (LVX), ciprofloxacin (CIP), sparfloxacin (SPX), and enoxacin (ENX) were purchased from LKT Laboratories, Inc. (St. Paul, MN); sitafloxacin (SIX) was from Daiichi Pharma-

* Corresponding author. Mailing address: Department of Global Epidemiology, Hokkaido University Research Center for Zoonosis Control, Kita 20-Nishi 10, Kita-ku, Sapporo 001-0020, Japan. Phone: 81-11-706-9503. Fax: 81-11-706-7310. E-mail: suzuki@czc.hokudai.ac.jp.

† Supplemental material for this article may be found at http://aac.asm.org/.

▽ Published ahead of print on 6 June 2011.

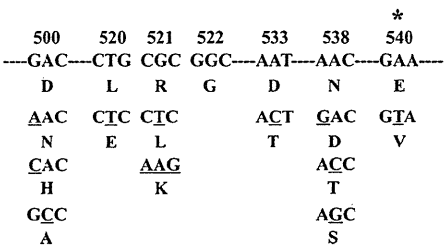

FIG. 1. Amino acid substitutions found within the QRDR of GyrB in FQ-resistant *M. tuberculosis*. The amino acid substitutions are shown below the nucleotide sequence. The target nucleotide substitution of this study is denoted by the asterisk, and mutated bases are underlined.

ceutical, Co., Ltd. (Tokyo, Japan); norfloxacin (NOR) was from Wako Pure Chemical Industries, Ltd. (Tokyo, Japan); moxifloxacin (MXF) was from Toronto Research Chemicals Inc. (Ontario, Canada); and ampicillin was from Meiji Seika Kaisha, Ltd. (Tokyo, Japan). Oligonucleotide primers were synthesized by Life Technologies (Carlsbad, CA). TOPO TA cloning (pCR 4-TOPO) and Ni-nitrilotriacetic acid protein purification kits were purchased from Life Technologies. Restriction enzymes were obtained from New England BioLabs, Inc. (Ipswich, MA). The supercoiling assay kit and supercoiled and relaxed pBR322 DNA were purchased from John Innes Enterprises Ltd. (Norwich, United Kingdom). Protease inhibitor cocktail (Complete Mini, EDTA free) was purchased from Roche Applied Science (Mannheim, Germany).

Bacterial strains and plasmids. *E. coli* strain TOP-10 (Life Technologies) was used as the host for cloning purposes. *E. coli* strains Rosetta-gami 2 and BL21(DE3)/pLysS were purchased from Merck KGaA (Darmstadt, Germany) and used for protein expression. Vector plasmids pET-20b (+) and pET-19b (Merck KGaA) were used to construct expression plasmids for *M. tuberculosis* proteins GyrA and GyrB, respectively.

Construction of wild-type (WT) and GyrB-E540V DNA gyrase expression vectors. The construction of WT DNA gyrase expression vectors is shown in Fig. S1 in the supplemental material. A nucleotide substitution was introduced into the *M. tuberculosis* WT *gyrB* gene by PCR with pairs of complementary primers containing the nucleotide substitution of interest (Table 1). The *gyrB*-M cassettes with mutated bases were amplified from the WT *gyrB* gene cassette (see Fig. S1C in the supplemental material) and ligated into the TA cloning plasmid. Recombinant plasmids were recovered from the colonies, and a nucleotide substitution in QRDRs in the 294-base PCR products was confirmed. The *gyrB*-M cassettes were digested with SacI and HindIII, ligated into pTB-B digested with same restriction endonucleases, and transformed into *E. coli* TOP-10 to obtain GyrB-E540V expression plasmids. Recombinant clones were selected from the resistant colonies on LB agar plates containing ampicillin (100 μg/ml).

Sequencing of products. PCR products were purified by agarose gel electrophoresis. The agarose blocks containing the bands of interest were sliced out of the agarose gel, frozen at −80°C for 30 min, and centrifuged at 20,400 × *g* at 4°C for 10 min to collect the supernatants. Supernatants having DNA concentrations between approximately 10 and 20 ng/μl were used directly as templates for cycle sequencing in both directions with corresponding primers (0.10 μmol) using the ABI Prism BigDye Terminator v3.1 cycle sequencing kit (Applied Biosystems, Foster City, CA). The sequencing reactions were performed according to the manufacturer's instructions. Cycle sequencing products were subsequently analyzed on an ABI PRISM 3130x automated genetic analyzer (Applied Biosystems). The sequences generated with the program were compared to their respective WT and GyrB-E540V sequences using BioEdit software.

Recombinant expression and purification of DNA gyrase. DNA gyrase subunits were purified as previously described, with the following modifications (1, 2). Expression vectors carrying the *gyrA* and *gyrB* genes of *M. tuberculosis* were transformed into *E. coli* Rosetta-gami 2 and BL21(DE3)/pLysS, respectively. Expression of GyrA and GyrB was induced with the addition of 1 mM isopropyl-β-D-thiogalactopyranoside (IPTG; Wako Pure Chemicals Ltd.), followed by further incubation at 14°C for 20 h or at 23°C for 5 h, respectively. Combined elution fractions resulting from the addition of elution buffer (20 mM Tris-HCl [pH 8.0], 500 mM NaCl, 250 mM imidazole) to nickel-nitrilotriacetic acid agarose resin (Invitrogen) were dialyzed twice overnight at 4°C against 1 liter of gyrase dilution buffer (50 mM Tris-HCl [pH 7.5], 100 mM KCl, 2 mM dithiothreitol, 1 mM EDTA). After dialysis, the eluates were added to glycerol to yield 50% (wt/vol) and stored at −80°C until use. The protein fractions were examined by sodium dodecyl sulfate (SDS)-polyacrylamide gel electrophoresis.

DNA supercoiling assay and inhibition by FQs. ATP-dependent DNA supercoiling and quinolone-inhibited supercoiling assays were carried out as previously described (1, 2, 25). DNA supercoiling activity was tested with a combination of purified *M. tuberculosis* GyrA and GyrB proteins. The reaction mixture (total volume, 30 μl) consisted of DNA gyrase assay buffer, relaxed pBR322 DNA (0.3 μg), and WT and GyrB-E540V gyrase proteins (3 μM). Reactions were run at 37°C for 1 h and stopped by the addition of 30 μl of chloroform-isoamyl alcohol (24:1 mixture) and 6 μl of 5× stop and loading solution. The total reaction mixtures were subjected to electrophoresis in 1% agarose gels in 0.5× Tris-borate-EDTA (TBE) buffer. The gels were run for 1 h at 50 mA and stained with ethidium bromide (0.7 μg/ml). *E. coli* DNA gyrase (John Innes Enterprises Ltd.) was used as a positive control for the assay procedures and buffer. The inhibitory effects of quinolones on DNA gyrase were assessed by determining the drug concentrations required to inhibit the supercoiling activity of the enzyme by 50% (IC_{50}s) in the presence or absence of serial 2-fold increases in the concentrations of the eight FQs. Supercoiling activity was assessed by tracing the brightness of the bands corresponding to the supercoiled pBR322 DNA with the Molecular Analyst software ImageJ (http://rsbweb.nih.gov/ij). To allow direct comparison, all incubations with WT and GyrB-E540V enzymes were carried out and processed in parallel on the same day under identical conditions. All enzyme assays were performed at least three times to confirm reproducibility.

Quinolone-mediated DNA cleavage assay. DNA cleavage assays were carried out as previously described (1, 2, 25). Supercoiled, rather than relaxed, pBR322 DNA was used as the substrate for cleavage assays. The reaction mixture (total volume, 30 μl) contained DNA gyrase assay buffer, purified DNA gyrase subunits, supercoiled pBR322 DNA (0.3 μg), and increasing concentrations of GAT, LVX, CIP, MXF, SPX, or SIX. After incubation for 1 h at 37°C, 3 μl of 2% SDS and 3 μl of proteinase K (1 mg/ml) were added to the reaction mixture. After additional incubation for 30 min at 37°C, reactions were stopped to allow relaxation activity by the addition of 3 μl of 0.5 mM EDTA, 30 μl of chloroform-

TABLE 1. Oligonucleotide sequences of primers used in PCR

Primer	Sequence (nucleotide position), underlined element(s)	Comment
ON-873	5′-CCCATATGACAGACACGACGTTGCCGCC-3′ (1–23), NdeI site	WT *gyrA*
ON-874	5′-GTTAACCGGGCTTCGGTGTACCTCATCG-3′ (377–404), HpaI site	WT *gyrA*
ON-875	5′-GGTTAACCCCGTTGGCGATGGAGATGC-3′ (398–424), HpaI site	WT *gyrA*
ON-876	5′-GGCTCGAGTTAATGATGATGATGATGATTGCCCGTCTGGTCTGCGCCG-3′ (2493–2517), XhoI site and 6-histidine tag, respectively	WT *gyrA*
ON-35	5′-CCCCCCCATATGGGTAAAAACGAGGCCAGAAG-3′ (1–23), NdeI site	WT *gyrB*
ON-882	5′-CACGAGCTCTCGTGCCTTACGTGCCGCGATACG-3′ (1366–1398), SacI site	WT *gyrB*
ON-883	5′-GAGAGCTCGTGCGGCGTAAGAGCGCCACCG-3′ (1388–1417)	WT *gyrB*
ON-884	5′-CGATCTTGTGGTAGCGAAGCTTGCCGATATCGA-3′ (1667–1699), HindIII site	WT *gyrB*
ON-885	5′-CGATATCGGCAAGCTTCGCTACCACAAGATCG-3′ (1668–1699)	WT *gyrB*
ON-886	5′-GGCTCGAGTTAGACATCCAGGAACCGAACATCC-3′ (2130–2145), XhoI site	WT *gyrB*
ON-40	5′-AAAGAACACC**GTA**GTTCAGGCGA-3′ (1607–1630)[a]	Mutant *gyrB*
ON-41	5′-TCGCCTGAAC**TAC**GGTGTTCTTT-3′ (1607–1630)[a]	Mutant *gyrB*

[a] Mutated codon shown in bold type.

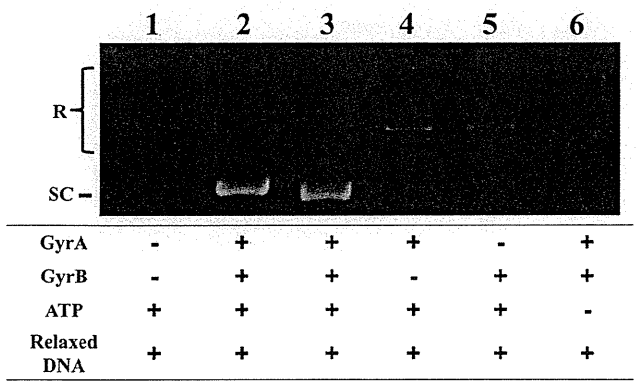

FIG. 2. Recombinant WT GyrA and GyrB subunits of *M. tuberculosis* generate an ATP-dependent DNA supercoiling activity. Relaxed pBR322 DNA (0.3 μg) was incubated with WT DNA gyrase reconstituted from GyrA (3 μM) and GyrB (3 μM) in the presence and absence of 1 mM ATP. The reactions were stopped, and the DNA products were separated by electrophoresis in 1% agarose gels. DNA was stained with ethidium bromide and photographed under UV illumination. Lane 1, relaxed pBR322 DNA; lane 2, relaxed pBR322 DNA and *E. coli* DNA gyrase; lane 3, relaxed pBR322 DNA and both recombinant GyrA and GyrB proteins; lane 4, relaxed pBR322 DNA and only GyrA protein; lane 5, relaxed pBR322 DNA and only GyrB protein; lane 6, absence of ATP. R and SC, relaxed and supercoiled pBR322 DNA, respectively.

isoamyl alcohol (24:1 mixture), and 3 μl of 10× DNA loading solution. Plasmid pBR322 linearized by BamHI digestion was used as a marker for cleaved DNA. The total reaction mixtures were subjected to electrophoresis in 0.8% agarose gels in 0.5× TBE buffer. The gels were run for 1.5 h at 50 mA, stained with ethidium bromide (0.7 μg/ml), and photographed under UV transillumination. The extent of DNA cleavage was quantified with the Molecular Analyst software ImageJ (http://rsbweb.nih.gov/ij). The quinolone concentrations required to induce 25% of the maximum DNA cleavage (CC_{25}s) were determined for the eight FQs.

RESULTS

Expression and purification of recombinant gyrase A and B proteins. The WT *gyrA* and *gyrB* genes were amplified from *M. tuberculosis* H37Rv (1, 2, 34). The full-length *gyrA* and *gyrB* genes were inserted downstream of the T7 promoter in expression vectors pET-20b (+) and pET19b, respectively, for expression as His-tagged recombinant proteins since the His tag has been previously shown not to interfere with the catalytic functions of GyrA and GyrB (14). Resulting plasmids pTB-A (*gyrA* in pET-20b) and pTB-B (*gyrB* in pET-19b) were used to transform *E. coli* Rosetta-gami 2 (DE3)/pLysS and BL21(DE3)/pLysS, respectively. Expression of the WT *gyrA* and *gyrB* genes in *E. coli* strains by induction with IPTG and subsequent purification of the corresponding proteins by Ni-nitrilotriacetic acid affinity purification resulted in 2 and 5 mg of soluble His-tagged 93-kDa and 79-kDa proteins from 200-ml cultures, respectively. We used mutagenesis of WT *gyrB* to introduce the desired amino acid substitution and purified the corresponding GyrB-E540V protein by the same procedure as that used for WT GyrB. All recombinant subunits were obtained at high purity (>95%) in milligram amounts (see Fig. S2 in the supplemental material) and free of contaminating *E. coli* topoisomerase activity, as assessed by the lack of supercoiling activity of either GyrA or GyrB alone (Fig. 2, lanes 4 and 5).

DNA supercoiling activity of WT and GyrB-E540V DNA gyrases. Combinations of the WT GyrA and GyrB subunits were examined for DNA supercoiling activity with relaxed pBR322 DNA as the substrate in the presence and absence of ATP (Fig. 2). A combination of GyrA and GyrB at 3 μM each was sufficient for the conversion of 100% of 0.3 μg of relaxed plasmid pBR322 DNA to its supercoiled form and was used for all DNA supercoiling experiments. Since the combination of the GyrA and GyrB subunits at 3 μM led to plasmid supercoiling in the presence of ATP, reconstituted DNA gyrase was considered functional (Fig. 2, lane 3). Neither subunit alone exhibited DNA supercoiling activity in the presence of 1 mM ATP (Fig. 2, lanes 4 and 5), and no supercoiling activity was observed when ATP was absent from the reaction mixture (Fig. 2, lane 6), indicating that both subunits and ATP were essential for DNA supercoiling activity. The activity of a GyrB-E540V enzyme (designated GyrB-E540V) was also determined by DNA supercoiling assay in the presence of complementary WT GyrA (see Fig. S3 in the supplemental material).

Determination of IC_{50}s of quinolones. The inhibitory effects of quinolones on the WT and GyrB-E540V enzymes were elucidated by quinolone-inhibited DNA supercoiling assay. A set of representative data showing the inhibitory effect of CIP is shown in Fig. 3, and data for the other FQs are presented in Fig. S4 in the supplemental material. Each of the quinolones showed dose-dependent inhibition of the WT and GyrB-E540V enzymes. Inhibitory effects of quinolones against recombinant gyrases are presented as IC_{50}s ordered from low to high in Table 2. The gyrase bearing the E540V amino acid substitution in GyrB was highly resistant to inhibition by quin-

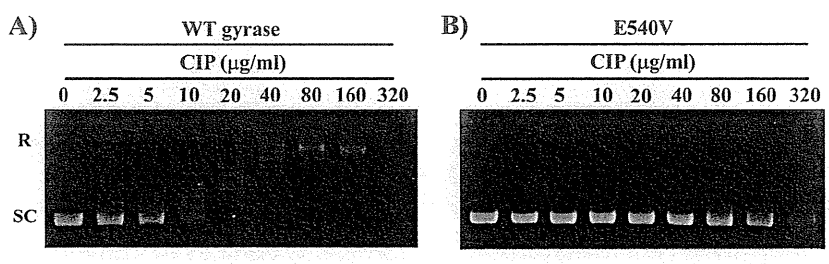

FIG. 3. Inhibitory activities of CIP on the supercoiling activities of WT and GyrB-E540V *M. tuberculosis* DNA gyrases. Relaxed pBR322 DNA (0.3 μg) was incubated with WT (A) or GyrB-E540V (B) DNA gyrase in the presence of the concentrations of CIP indicated. The reactions were stopped, and the DNA products were analyzed by electrophoresis in 1% agarose gels. R and SC denote relaxed and supercoiled pBR322 DNA, respectively.

TABLE 2. IC_{50}s and CC_{25} of FQs against WT and mutant DNA gyrases[a]

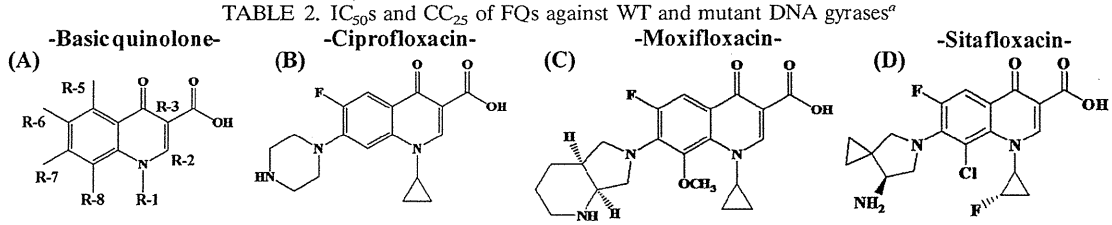

Quinolone	Substituent			IC_{50} (μg/ml)			CC_{25} (μg/ml)		
	R-1	R-7	R-8	WT	E540V	Ratio	WT	E540V	Ratio
SIX	Fluorinated cyclopropyl	Pyrrolidine	Cl	4	10	2.5	2	3	1.5
GAT	Cyclopropyl	Piperazine	O-CH_3	9	37	4.1	7	26	3.7
SPX	Cyclopropyl	Piperazine	F	7	52	7.4	10	37	3.7
MXF	Cyclopropyl	Azabicyclo	O-CH_3	16	61	3.8	5	17	3.4
LVX	Bridge N1-C8	Piperazine	Bridge N1-C8	22	82	3.7	25	57	2.3
CIP	Cyclopropyl	Piperazine	H	7	251	35.9	23	317	13.8
NOR	Ethyl	Piperazine	H	102	274	2.7	NO[b]	NO	NO
ENX	Ethyl	Piperazine	N	84	>320	>3.8	NO	NO	NO

[a] The structures of the compounds used (A, basic quinolone; B, CIP; C, MXF; D, SIX) and the locations of the substituents are shown at the top.
[b] NO, not observed.

olones (Fig. 3; Table 2; see Fig. S4 in the supplemental material). The IC_{50} of SIX was 10 μg/ml, those of GAT, LVX, MXF, and SPX were 37 to 82 μg/ml, and those of CIP, NOR, and ENX were 251, 274, and >320 μg/ml, respectively.

Quinolone-mediated DNA cleavage complex formation by WT and GyrB-E540V DNA gyrase. To examine the effects of FQs on cleavage complex formation by WT and GyrB-E540V DNA gyrase, cleavage assays were performed in which supercoiled pBR322 was incubated with WT or GyrB-E540V DNA gyrase in the presence or absence of increasing concentrations of quinolones. Figure 4 shows the results of a representative cleavage assay using CIP. Table 2 presents the CC_{25}s of the other FQs. The CC_{25}s of FQs for WT gyrase ranged from 2 to 25 μg/ml, while those for the GyrB-E540V enzyme ranged from 3 to 317 μg/ml (Table 2).

DISCUSSION

In light of the increased demand for a new treatment regimen for MDR TB, FQs have started to be used as anti-TB agents (13, 20). Although the main target of FQs is known to be bacterial DNA gyrase, the molecular details of quinolone-gyrase interactions are not yet fully understood. In this study, we examined the E540V amino acid substitution we recently found in a clinical isolate from Bangladesh (unpublished data). The same amino acid substitution has also been reported in a clinical isolate from Vietnam (12). Even though the E540 residue of GyrB, equivalent to the E466 residue in *E. coli*, has been suggested to be located in the QRDR in *M. tuberculosis* by X-ray crystallography (28), there was no experimental confirmation of this. We examined the effect of the amino acid substitution on FQ resistance at the molecular level by using purified recombinant gyrase subunits. Supercoiling and cleavage assays in the presence of several FQs demonstrated the significant contribution of the E540V amino acid substitution to quinolone resistance (Fig. 2 and 3; Table 2; see Fig. S3 and S4 in the supplemental material). These results support the model proposed by Piton et al. (28).

The structure-activity relationship between FQs and WT and GyrB-E540V gyrases were analyzed. All eight FQs studied have a substituent, pyrrolidine, piperazine, or azabicyclo, at R-7 which has been suggested to be associated with E540 on GyrB (28). NOR and ENX, with an ethyl residue at R-1, have high IC_{50}s (102 and 84 μg/ml, respectively), whereas the other FQs, with a cyclopropyl at R-1 or an N1-C8 bridge, have significantly lower IC_{50}s (4 to 22 μg/ml) for WT gyrase, suggesting that a cyclopropyl at R-1 or an N1-C8 bridge contributes to FQ activity. Although higher IC_{50}s of all FQs were observed for the GyrB-E540V enzyme than for the WT en-

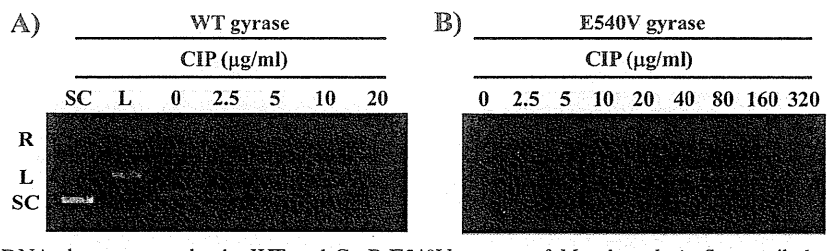

FIG. 4. CIP-mediated DNA cleavage complex by WT and GyrB-E540V gyrases of *M. tuberculosis*. Supercoiled pBR322 DNA (0.3 μg) was incubated with WT (A) or GyrB-E540V (B) DNA gyrase in the presence of the concentrations of CIP indicated. After addition of SDS and protease K, the reactions were stopped and the mixture samples were analyzed by electrophoresis in 0.8% agarose gels. R, L, and SC denote relaxed, BamHI-linearized, and supercoiled pBR322 DNA, respectively.

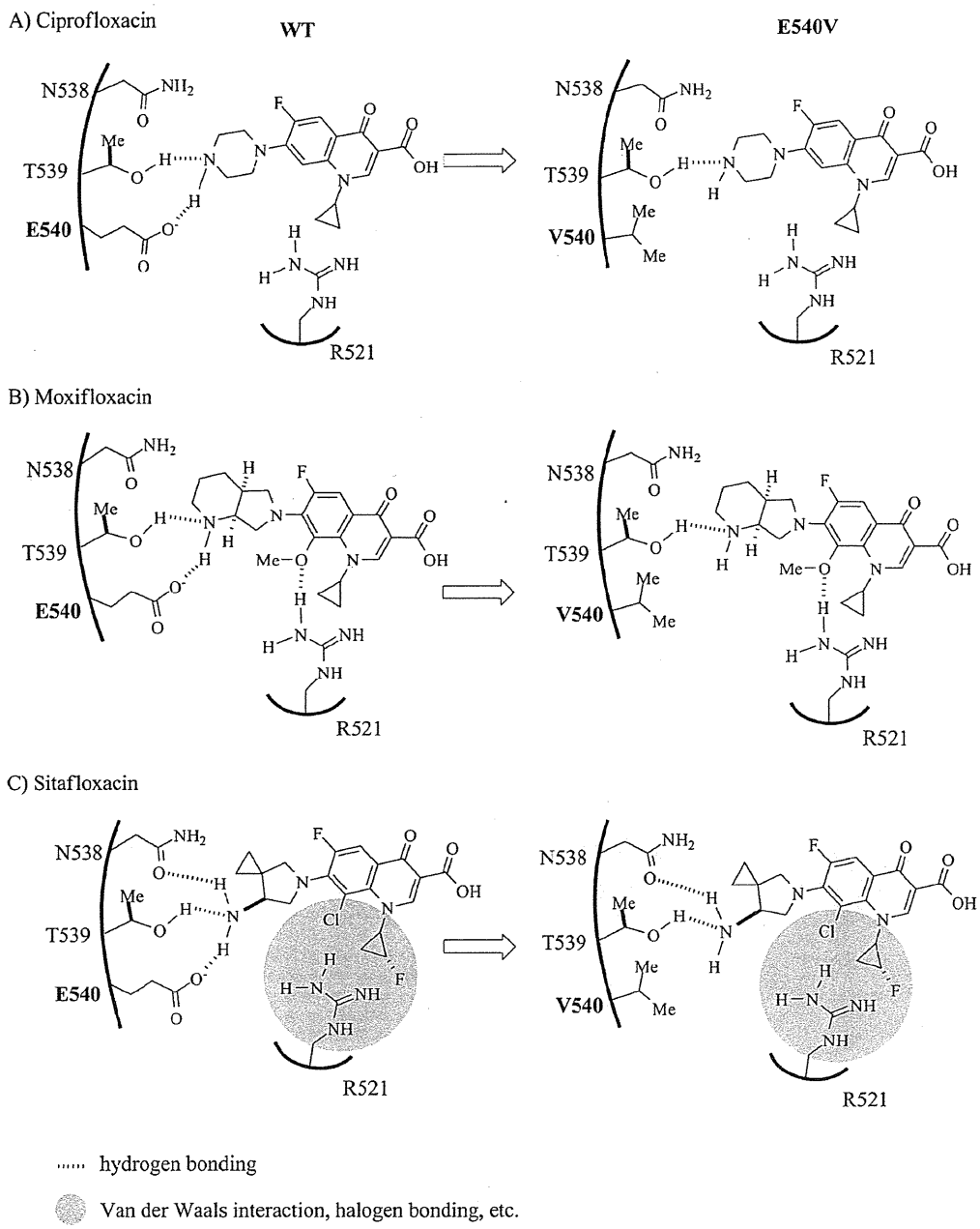

FIG. 5. Hypothetical models of interactions of WT and E540V GyrB with quinolones with substituents at R-7 and R-8. The models show the hydrogen bonding network relationship between residues of the WT and E540V gyrases and the R-7 and R-8 groups of CIP (A). Panels B and C show the relationships of MXF and SIX with the QBP of the DNA GyrB subunit of *M. tuberculosis*. The left and right panels show the WT and GyrB-E540V gyrase activities for hydrogen interaction with quinolones. Position 540 is indicated by bold type.

zyme, the difference in the two IC_{50}s was lowest for SIX. In particular, this FQ has a fluorinated cyclopropyl ring at R-1 while four other FQs, GAT, SPX, MXF, and CIP, have a cyclopropyl. In contrast, the difference between the CIP IC_{50}s for the E540V and WT enzymes was significantly high. The only apparent difference between CIP and the other effective FQs was the absence of a substituent at R-8 (Table 2). We have also attempted to elucidate the effects of the E540V amino acid substitution in GyrB using DNA cleavage assays (Fig. 4 and Table 2) to confirm the results obtained by quinolone-inhibited supercoiling assays.

Amino acid residues in GyrB located close to E540 (E501 in reference 28), including N538 (N499) and T539 (T500) on the α2 helix and R482 (R521) on β2, have been proposed to interact with the GyrA subunit and DNA strands to form the QBP (28). It has been suggested that the β1-α1 loop (residues 498 to 501 in GyrB of *M. tuberculosis*) interacts with the R-1 group, the β2-DBL (DNA-binding loop, residues 519 to 525)

interacts with the R-7 and R-8 groups, and the beginning of α2 (residues 537 to 541) interacts with the R-7 group (28). A substitution of the glutamic acid at position 540 with a valine may therefore lead to a conformational change in QBP geometry in GyrB (28).

Based on the crystal structure and current data obtained with several FQs (5, 16, 28), we hypothesize the mechanism of FQ resistance conferred by the E540V amino acid substitution on GyrB as shown in Fig. 5. The hydrogen bonding network involving E540 could play a pivotal role in the recognition of quinolones by the GyrB subunit on QBP. One of the FQs, CIP, exerts potent inhibitory activity against WT DNA gyrase (IC_{50} = 7 μg/ml) and may bind tightly to GyrB through two hydrogen bonds (O-H—N and O^-—H-N) involving a hydroxyl group (OH) of the T539 residue and a carboxylate (CO_2-) of the E540 residue (Fig. 5A, left; Table 2). In contrast, the efficacy of CIP against the GyrB-E540V gyrase is drastically lower (IC_{50} = 251 μg/ml). The E540V amino acid substitution replaces glutamic acid, which bears a carboxyl group, with valine, which is nonpolar and sterically demanding. The subsequent loss of the hydrogen bonding interactions with E540 could induce a substantial conformational change, which would disrupt binding with CIP (Fig. 5A, right). The efficacy of other FQs carrying a substituent at R-8 against the E540V enzyme was shown to be higher than that of CIP (Table 2). For example, MXF showed inhibitory activities against WT GyrB and E540V GyrB, with IC_{50}s of 16 and 61 μg/ml, respectively. MXF and CIP vary structurally with regard to the substituents at R-7 and R-8: MXF has a bulky azabicyclo group at R-7 and a methoxy group at R-8, whereas CIP has a simple piperazine group at R-7 and no substituent at R-8 (Table 2). In the binding of MXF with WT GyrB (Fig. 5B, left), the substituents at R-7 and R-8 may efficiently interact with residues of the GyrB subunit through three hydrogen bonding networks involving T539 (O-H—N), E540 (O^-—H-N), and R521 (H-N-H—O-Me). With regard to the GyrB E540V gyrase (Fig. 5B, right), however, MXF could still retain a substantial affinity for the GyrB subunit through hydrogen bonding with the substituents at R-7 and R-8 (O-H—N and H-N-H—O-Me), whereas CIP could not retain such an affinity due to the absence of hydrogen bonding with the substituent at R-8 and would thus be more sensitive to the amino acid substitution. Apart from MXF and CIP, SIX carries a pyrrolidine at R-7 and a halide (chlorine) at R-8 and exhibits potent activities toward the WT (IC_{50} = 4 μg/ml) and GyrB-E540V (IC_{50} = 10 μg/ml) gyrase enzymes. As shown in Fig. 5C, the substituents at R-7 and R-8 of SIX may interact with the residues of the WT GyrB subunit through three hydrogen bonds and van der Waals forces and/or halogen bonding (4) involving T539 (O-H—N), E540 (O^-—H-N), N538 (O-O—H-N), and R521 (van der Waals radius zone between residue R521 and the R-8 halide group). It seems likely that interactions between R521 and the substituents at R-1 and R-8 are sufficient to make up for the loss of hydrogen bonding with the GyrB-E540V gyrase and thus play important roles in the binding of SIX.

In summary, our study indicates that the E540V amino acid substitution in GyrB is involved in the resistance of *M. tuberculosis* against quinolones, although E540 is reported to be outside GyrB QRDRs. We thus propose that the E540 residue be included in the QRDR in *M. tuberculosis* as shown in *Streptococcus pneumoniae* (23, 26). Moreover, we also demonstrated an association between structural features of quinolones and activities against the WT and E540V forms of the GyrB DNA gyrase subunit of *M. tuberculosis*. The interaction between FQs and GyrB, which is composed of hydrogen bonding networks involving substituents of FQs and amino acid residues of QBP in GyrB, plays an important role in the inhibitory activity of FQs. Further studies investigating the contributions of other amino acid substitutions may also help gain a comprehensive understanding of the mechanism by which FQ-resistant TB emerges.

ACKNOWLEDGMENTS

We thank Haruka Suzuki, Yukari Fukushima, and Aiko Ohnuma for their technical support with several of the experiments and Yusuke Suzuki and Kyeong Hwa Bae for their helpful comments.

This work was supported by a grant from U.S.-Japan Cooperative Medical Science Programs, the Global Center of Excellence (COE) Program, Establishment of International Collaboration Centers for Zoonosis Control, Ministry of Education, Culture, Sports, Science, and Technology (MEXT), Japan, in part by J-GRID, the Japan Initiative for Global Research Network on Infectious Diseases from MEXT to Y.S., and by Grants-in-Aid for Scientific Research from the Japan Society for the Promotion of Science (JSPS) to Y.S. and C.N.

REFERENCES

1. **Aubry, A., X. S. Pan, L. M. Fisher, V. Jarlier, and E. Cambau.** 2004. *Mycobacterium tuberculosis* DNA gyrase: interaction with quinolones and correlation with antimycobacterial drug activity. Antimicrob. Agents Chemother. **48:**1281–1288.
2. **Aubry, A., et al.** 2006. Novel gyrase mutations in quinolone-resistant and -hypersusceptible clinical isolates of *Mycobacterium tuberculosis*: functional analysis of mutant enzymes. Antimicrob. Agents Chemother. **50:**104–112.
3. **Aziz, M. A., et al.** 2006. Epidemiology of antituberculosis drug resistance (the Global Project on Anti-tuberculosis Drug Resistance Surveillance): an updated analysis. Lancet **368:**2142–2154.
4. **Barnard, F. M., and A. Maxwell.** 2001. Interaction between DNA gyrase and quinolones: effects of alanine mutations at GyrA subunit residues Ser^{83} and Asp^{87}. Antimicrob. Agents Chemother. **45:**1994–2000.
5. **Bax, B. D., et al.** 2010. Type IIA topoisomerase inhibition by a new class of antibacterial agents. Nature **466:**935–940.
6. **Blumberg, H. M., et al.** 2003. American Thoracic Society/Centers for Disease Control and Prevention/Infectious Diseases Society of America: treatment of tuberculosis. Am. J. Respir. Crit. Care Med. **167:**603–662.
7. **Champoux, J. J.** 2001. DNA topoisomerases: structure, function, and mechanism. Annu. Rev. Biochem. **70:**369–413.
8. **Cole, S. T., et al.** 1998. Deciphering the biology of *Mycobacterium tuberculosis* from the complete genome sequence. Nature **393:**537–544.
9. **Corbett, K. D., and J. M. Berger.** 2004. Structure, molecular mechanisms, and evolutionary relationships in DNA topoisomerases. Annu. Rev. Biophys. Biomol. Struct. **33:**95–118.
10. **Drlica, K.** 1999. Mechanisms of fluoroquinolone action. Curr. Opin. Microbiol. **2:**504–508.
11. **Drlica, K., and X. Zhao.** 1997. DNA gyrase, topoisomerase IV, and the 4-quinolones. Microbiol. Mol. Biol. Rev. **61:**377–392.
12. **Duong, D. A., et al.** 2009. Beijing genotype of *Mycobacterium tuberculosis* is significantly associated with high-level fluoroquinolone resistance in Vietnam. Antimicrob. Agents Chemother. **53:**4835–4839.
13. **Fattorini, L., et al.** 1999. Activity of 16 antimicrobial agents against drug-resistant strains of *Mycobacterium tuberculosis*. Microb. Drug Resist. **5:**265–270.
14. **Freydank, A. C., W. Brandt, and B. Dräger.** 2008. Protein structure modeling indicates hexahistidine-tag interference with enzyme activity. Proteins **72:**173–183.
15. **Frieden, T. R., et al.** 1993. The emergence of drug-resistant tuberculosis in New York City. N. Engl. J. Med. **328:**521–526.
16. **Fu, G. S., et al.** 2009. Crystal structure of DNA gyrase B′ domain sheds lights on the mechanism for T-segment navigation. Nucleic Acids Res. **37:**5908–5916.
17. **Gillespie, S. H., and N. Kennedy.** 1998. Fluoroquinolones: a new treatment for tuberculosis? Int. J. Tuberc. Lung Dis. **2:**265–271.
18. **Gore, J., et al.** 2006. Mechanochemical analysis of DNA gyrase using rotor bead tracking. Nature **439:**100–104.
19. **Guillemin, I., V. Jarlier, and E. Cambau.** 1998. Correlation between quinolone susceptibility patterns and sequences in the A and B subunits of DNA gyrase in mycobacteria. Antimicrob. Agents Chemother. **42:**2084–2088.

20. **Hatfull, G. F., and W. R. Jacobs, Jr.** 2000. Molecular genetics of mycobacteria, p. 235–256. American Society for Microbiology, Washington, DC.
21. **Heeb, S., et al.** 2011. Quinolones: from antibiotics to autoinducers. FEMS Microbiol. Rev. **35:**247–274.
22. **Infectious Diseases Society of the Republic of China; Society of Tuberculosis, Taiwan; Medical Foundation in Memory of Deh-Lin Cheng; Foundation of Wei-Chuan Hsieh for Infectious Diseases Research and Education; C Y Lee's Research Foundation for Pediatric Infectious Diseases and Vaccines.** 2004. Guidelines for chemotherapy of tuberculosis in Taiwan. J. Microbiol. Immunol. Infect. **37:**382–384.
23. **Laponogov, I., et al.** 2010. Structural basis of gate-DNA breakage and resealing by type II topoisomerases. PLoS One **5:**e11338.
24. **Levine, C., H. Hiasa, and K. J. Marians.** 1998. DNA gyrase and topoisomerase IV: biochemical activities, physiological roles during chromosome replication, and drug sensitivities. Biochim. Biophys. Acta **1400:**29–43.
25. **Pan, X. S., G. Yague, and L. M. Fisher.** 2001. Quinolone resistance mutations in *Streptococcus pneumoniae* GyrA and ParC proteins: mechanistic insights into quinolone action from enzymatic analysis, intracellular levels, and phenotypes of wild-type and mutant proteins. Antimicrob. Agents Chemother. **45:**3140–3147.
26. **Pan, X. S., K. A. Gould, and L. M. Fisher.** 2009. Probing the differential interactions of quinazolinedione PD 0305970 and quinolones with gyrase and topoisomerase IV. Antimicrob. Agents Chemother. **53:**3822–3831.
27. **Pitaksajjakul, P., et al.** 2005. Mutations in the *gyrA* and *gyrB* genes of fluoroquinolone-resistant *Mycobacterium tuberculosis* from TB patients in Thailand. Southeast Asian J. Trop. Med. Public Health **36**(Suppl. 4)**:**228–237.
28. **Piton, J., et al.** 2010. Structural insights into the quinolone resistance mechanism of *Mycobacterium tuberculosis* DNA gyrase. PLoS One **5:**e12245.
29. **Reece, R. J., and A. Maxwell.** 1991. DNA gyrase: structure and function. Crit. Rev. Biochem. Mol. Biol. **26:**335–375.
30. **Sepkowitz, K. A., E. E. Telzak, S. Recalde, and D. Armstrong.** 1994. Trend in the susceptibility of tuberculosis in New York City, 1987-1991. Clin. Infect. Dis. **18:**755–759.
31. **Sharma, S. K., and A. Mohan.** 2004. Multidrug-resistant tuberculosis. Indian J. Med. Res. **120:**354–376.
32. **Sun, Z., et al.** 2008. Comparison of *gyrA* gene mutations between laboratory-selected ofloxacin-resistant *Mycobacterium tuberculosis* strains and clinical isolates. Int. J. Antimicrob. Agents **31:**115–121.
33. **Takiff, H. E., et al.** 1994. Cloning and nucleotide sequence of *Mycobacterium tuberculosis gyrA* and *gyrB* genes and detection of quinolone resistance mutations. Antimicrob. Agents Chemother. **38:**773–780.
34. **Veziris, N., et al.** 2007. Treatment failure in a case of extensively drug-resistant tuberculosis associated with selection of a GyrB mutant causing fluoroquinolone resistance. Eur. J. Clin. Microbiol. Infect. Dis. **26:**423–425.
35. **World Health Organization.** 2010. Multidrug and extensively drug-resistant TB (M/XDR-TB). Global report on surveillance and response. Document WHO/HTM/TB/2010.3. World Health Organization, Geneva, Switzerland.
36. **World Health Organization.** 2010. Global tuberculosis control: WHO report. Document WHO/HTM /TB/2010.7. World Health Organization, Geneva, Switzerland.
37. **World Health Organization.** 2008. Guidelines for the programmatic management of drug-resistant tuberculosis. WHO/HTM/TB/2008.402. World Health Organization, Geneva, Switzerland.
38. **World Health Organization.** 2008. Anti-tuberculosis drug resistance in the world fourth global report. The WHO/IUATLD Global Project on Anti-tuberculosis Drug Resistance Surveillance 2002-2007 WHO/HTM/TB/2008.394. World Health Organization, Geneva, Switzerland.
39. **Zhou, J., et al.** 2000. Selection of antibiotic-resistant bacterial mutants: allelic diversity among fluoroquinolone-resistant mutations. J. Infect. Dis. **182:**517–525.
40. **Zignol, M., et al.** 2006. Global incidence of multidrug-resistant tuberculosis. J. Infect. Dis. **194:**479–485.

Jpn. J. Infect. Dis., 65, 72-74, 2012

Short Communication

Influence of Lineage-Specific Amino Acid Dimorphisms in GyrA on *Mycobacterium tuberculosis* Resistance to Fluoroquinolones

Hyun Kim[1], Chie Nakajima[1], Youn Uck Kim[2], Kazumasa Yokoyama[1], and Yasuhiko Suzuki[1,3]*

[1]*Division of Global Epidemiology, Hokkaido University Research Center for Zoonosis Control, Sapporo 001-0020;*
[3]*JST/JICA-SATREPS, Tokyo 120-8666, Japan; and*
[2]*Department of Biomedical Sciences, Sun Moon University, A-San 336-708, Republic of Korea*

(Received September 14, 2011. Received October 31, 2011)

SUMMARY: We conducted in vitro DNA supercoiling assays, utilizing recombinant DNA gyrases, to elucidate the influence of the lineage-specific serine or threonine residue at position 95 of GyrA on fluoroquinolone resistance in *Mycobacterium tuberculosis*. There was little effect of the GyrA-Ala74Ser amino acid substitution on activity of the GyrA-Ser95 gyrase, while activity of the GyrA-Asp94Gly-Ser95 gyrase was reduced. These findings were in striking contrast to previous reports analyzing GyrA with Thr95 and suggest an important impact of the amino acid in the development of fluoroquinolone resistance.

The emergence of multidrug-resistant tuberculosis (MDR-TB) is a significant public health problem that poses a serious threat to global TB control (1). As a result, the need for novel classes of anti-TB drugs has increased, with fluoroquinolones (FQs) becoming the drug of choice for use in MDR-TB treatment (2–5).

FQs are a series of synthetic antimicrobial agents that inhibit bacterial DNA gyrase and topoisomerase IV (6–8). Although most bacteria are known to have both enzymes, *Mycobacterium tuberculosis* lacks topoisomerase IV (4–7), and thus, the sole target of FQs in *M. tuberculosis* is DNA gyrase.

The mechanism underlying development of FQ resistance in *M. tuberculosis* appears to involve amino acid substitutions in the quinolone resistance-determining regions (QRDRs) of the A or B subunit of DNA gyrase. These substitutions, which occur mainly at positions 88, 90, 91, and 94 in GyrA, and at positions 500, 521, and 540 in GyrB, have been shown to imbue *M. tuberculosis* with FQ resistance (9–14). In contrast, the polymorphism at position 95 in GyrA, which encodes a serine or threonine, has been shown to have no influence on FQ-resistance. Hence, these residues are considered to be lineage-specific amino acids. Recently, double mutations at codons 74 and 94 in GyrA QRDRs, causing amino acid substitutions from alanine to serine (Ala74Ser) and Asp94Gly, respectively, were reported in clinical isolates with high-level FQ-resistance in China (14,15). The majority of these isolates belong to the Beijing lineage, carrying the lineage-specific amino acid, threonine, at position 95 in GyrA. In addition, evidence that Ala74Ser enables development of FQ resistance was demonstrated using recombinant DNA gyrase constructed from genomic DNA of a *M. tuberculosis* clinical isolate, also bearing the GyrA-Thr95 polymorphism (17). Interestingly, no FQ-resistant clinical isolates carrying the Ala74Ser mutation have been reported in lineages also carrying GyrA-Ser95.

Here, in order to elucidate the influence of lineage-specific amino acid dimorphisms in GyrA on FQ resistance, we conducted in vitro DNA supercoiling inhibition assays utilizing recombinant DNA gyrases bearing a GyrA-Ser95 residue and its derivatives.

We constructed recombinant DNA gyrase expression plasmids using genomic DNA from *M. tuberculosis* H37Rv expressing Ser95 in GyrA, as described previously (12). Ala74Ser, Asp94Gly, and Ala74Ser-Asp94Gly mutations were introduced into the Ser95 *gyrA* DNA by PCR using pairs of complementary primers containing the mutations of interest (Table 1). Plasmid vectors, pET-20b (+) and pET-19b (Merck KGaA, Darmstadt, Germany) were used to construct 6 × His-tagged *M. tuberculosis* GyrA and GyrB expression plasmids. Expression of GyrA and GyrB in *Escherichia coli* Rosetta-gami 2 and BL21 (DE3) pLysS (Merck KGaA) was induced by treatment with 1 mM isopropyl β-D-1-thio-galactopyranoside (IPTG) at 14°C for 20 h, or at 23°C for 5 h.

Recombinant DNA gyrase subunits in sonicated *E. coli* lysates were trapped on nickel-nitrilotriacetic acid agarose resin (Invitrogen Corp., Carlsbad, Calif., USA) and were eluted with elution buffer (20 mM Tris-HCl [pH 8.0], 500 mM NaCl, and 250 mM imidazole). Eluates were dialyzed twice overnight at 4°C against 1 L gyrase dilution buffer (50 mM Tris-HCl [pH 7.5], 100 mM KCl, 2 mM DTT, 1 mM EDTA), an equal volume of glycerol was added, and samples were used for subsequent assays. The inhibitory effects of FQs on DNA gyrases were assessed by carrying out supercoiling inhibition assays in the presence or absence of increasing concentrations of three different FQs purchased from LKT Laboratories, Inc. (St. Paul, Minn., USA): gatifloxacin (GAT), levofloxacin (LVX), and ciprofloxacin (CIP).

*Corresponding author: Mailing address: Division of Global Epidemiology, Hokkaido University Research Center for Zoonosis Control, Kita 20-Nishi 10, Kita-ku, Sapporo 001-0020, Japan. Tel: +81-11-706-9503, Fax: +81-11-706-7310, E-mail: suzuki@czc.hokudai.ac.jp

Table 1. Nucleotide sequence of primers used for introducing amino acid substitutions

Primer name	Sequence (nucleotide position)	Amino acid substitutions to be introduced
ON-001	5′-CGCC AAG TCG TCC CGG TCG GTTG-3′ (210–232)	Ala74Ser *gyrA*
ON-002	5′-CAAC CGA CCG GGA CGA CTT GGCG-3′ (210–232)	Ala74Ser *gyrA*
ON-015	5′-GTCG ATC TAC GGC AGC CTG GTGC-3′ (270–292)	Asp94Gly *gyrA*
ON-016	5′-GCAC CAG GCT GCC GTA GAT CGAC-3′ (270–292)	Asp94Gly *gyrA*
ON-031	5′-GCAACTACCACCCGCACGGC-3′ (245–264)	Ala74Ser-Asp94Gly *gyrA*
ON-032	5′-GCCGTGCGGGTGGTAGTTGC-3′ (245–264)	Ala74Ser-Asp94Gly *gyrA*

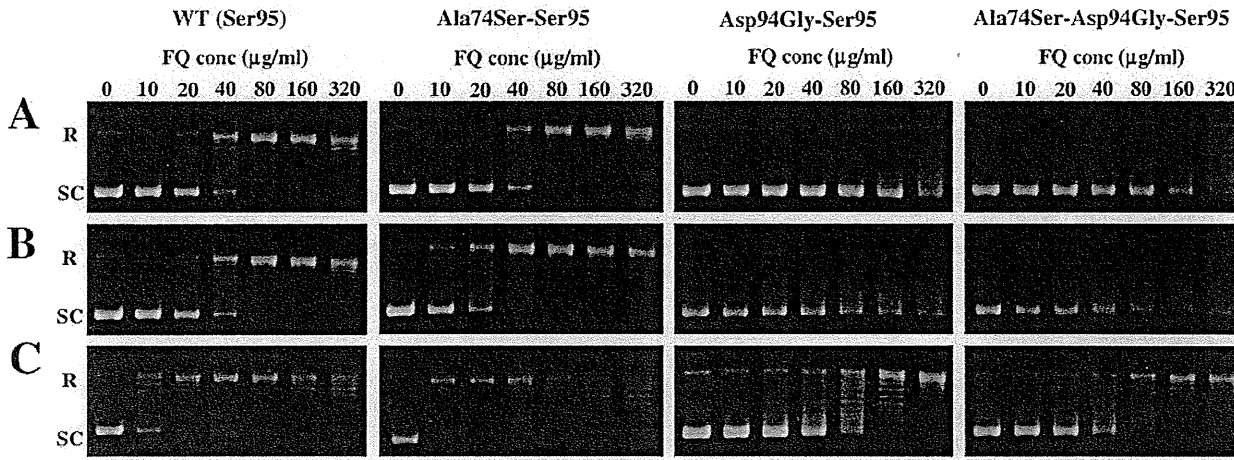

Fig. 1. Fluoroquinolones inhibited DNA supercoiling in assay. Relaxed pBR322 DNA (0.3 μg) was incubated with 3 μM of wild type (WT) or mutant GyrA and 3 μM of GyrB in the presence or absence of the indicated amounts (in μg/ml) of quinolones. A, levofloxacin; B, ciprofloxacin; and C, gatifloxacin at 37°C for 60 min. After stopping the reaction by adding equal volume of chloroform: isoamyl alcohol (24:1), DNA products in aqueous phase were analyzed by electrophoresis in a 1% agarose gel. R and SC indicate relaxed and supercoiled DNA, respectively.

Table 2. IC_{50} of FQs against wild type and mutant DNA gyrases

Quinolone	IC_{50}[1] (μg/ml)						Reference
	WT H37Rv (Ser95)	Ser95Thr	Ala74Ser-Ser95	Ala74Ser-Ser95Thr	Asp94Gly-Ser95	Ala74Ser-Asp94Gly-Ser95	
LVX	34		34		310	171	This work
CIP	18		17		196	107	
GAT	9		7		76	48	
OFX	1.92	3.30		15.56			Lau et al. (17)
MXF	0.98	1.62		14.37			

[1]: IC_{50}: half maximal inhibitory concentrations.
WT, wild type; LVX, levofloxacin; CIP, ciprofloxacin; GAT, gatifloxacin; OFX, ofloxacin; MXF, moxifloxacin.

Drug concentrations required to inhibit the supercoiling activity of the enzyme by 50% (IC_{50} values) were calculated using a formula developed by plotting amounts of supercoiled DNA against FQ concentration, as described previously (6,9,12,16).

Each of the FQ dose-dependently inhibited DNA supercoiling activity with IC_{50} values ranging from 7 to 310 μg/ml (Fig. 1 and Table 2). Wild type (GyrA-Ser95) and GyrA-Ala74Ser-Ser95 demonstrated similar levels of in vitro FQ susceptibility, implying that there is little influence of the GyrA-Ala74Ser amino acid substitution on inducing resistance against FQs. This is in striking contrast to data reported by Lau et al. (17). They noted 8.1- and 14.7-fold increases in resistance to ofloxacin (OFX) and moxifloxacin (MXF), respectively, for DNA gyrase with a GyrA-Ala74Ser substitution compared to that without this substitution in GyrA-Thr95 (Table 2).

The discrepancy between our present findings and those of Lau et al. suggests that Ala74Ser substitution affects FQ resistance only when there is a threonine at position 95 of GyrA. The amino acid at position 74 has been suggested to exist in the α3-helix domain, while that at position 95 is in the α4-helix domain (17–19). In addition, the Ala74Ser amino acid substitution has been hypothesized to perturb the GyrA-GyrA dimer interface by interrupting hydrophobic interactions between the two α3-helix domains, thereby contributing to FQ resistance (17). Our data suggest a possible role for the threonine methyl group at position 95 in this phenomenon by causing altered interactions between α4- and α3-helices, or other nearby structures, followed by induction of conformational changes in the quinolone-bind-

ing pocket (QBP).

Furthermore, we found that the IC_{50} values of LVX, CIP, and GAT against DNA gyrase with GyrA-Asp94Gly-Ser95 were 2-fold greater than those against DNA gyrase with GyrA-Ala74Ser-Asp94Gly-Ser95 (Table 2). In contrast, two previous studies have reported that Ala74Ser enhances FQ resistance. Shi et al. analyzed OFX-resistant clinical isolates and showed that Ala74Ser-Asp94Gly substitutions in GyrA were associated with a relatively high MIC for OFX, ranging from 2 to 32 μg/ml, whereas GyrA-Asp94Gly had a relatively low MIC, ranging from 1 to 4 μg/ml (15). Similarly, Sun et al. reported that the MICs of OFX against clinical isolates ranged from 4 to 20 μg/ml for those with GyrA-Ala74Ser-Asp94Gly, and from 1 to 10 μg/ml for those with GyrA-Asp94Gly (14). Since Aubry et al. demonstrated a significant correlation (R^2 = 0.9) between IC_{50} values for DNA gyrase and the MICs of FQs (6), the striking contrast between the findings of the two previous publications and our current data regarding the influence of GyrA-Ala74Ser and GyrA-Asp94Gly in GyrA-Ser95 suggests that the threonine at position 95 may enhance resistance by altering interactions between the α4- and α3-helices, or other structures. Furthermore, the high level of FQ resistance found in the Beijing genotype reported from Vietnam (20), which also carries a threonine at position 95, suggests an influence of lineage-specific amino acid residues on the acquisition of enhanced resistance.

In conclusion, the lineage-specific amino acid residue at position 95 in GyrA enables the acquisition of high-level resistance in *M. tuberculosis* against FQs, likely by inducing conformational changes in the QBP. Further studies of *M. tuberculosis* resistance, with various combinations of amino acid substitutions in DNA gyrases, are needed to confirm these observations.

Acknowledgments We thank Ms. Haruka Suzuki, Ms. Yukari Fukushima, and Ms. Aiko Ohnuma for their technical support, and Ms. Kyeong Hwa Bae for her helpful comments.

This work was supported by grants from the U.S.-Japan Cooperative Medical Science Program, the Global Center of Excellence Program, the "Establishment of International Collaboration Centers for Zoonosis Control", and the Ministry of Education, Culture, Sports, Science and Technology (MEXT), Japan; and in part by grants from the Japan Initiative for Global Research Network on Infectious Diseases MEXT to YS and by Grants-in-Aid for Scientific Research from Japan Society for the Promotion of Science to YS and CN.

Conflict of interest None to declare.

REFERENCES

1. World Health Organization (2010): Multidrug and Extensively Drug-Resistant TB (M/XDR-TB): 2010 Global Report on Surveillance and Response. WHO/HTM/TB/2010.3. World Health Organization, Geneva, Switzerland.
2. Blumberg, H.M., Burman, W.J., Chaisson, R.E., et al. (2003): American Thoracic Society/Centers for Disease Control and Prevention/Infectious Diseases Society of America: treatment of tuberculosis. Am. J. Respir. Crit. Care Med., 167, 603–662.
3. Chakravorty, S., Aladegbami, B., Thoms, K., et al. (2011): Rapid detection of fluoroquinolone-resistant and heteroresistant *Mycobacterium tuberculosis* by use of sloppy molecular beacons and dual melting-temperature codes in a real-time PCR assay. J. Clin. Microbiol., 49, 932–40.
4. Ginsburg, A.S., Grosset, J.H. and Bishai, W.R. (2003): Fluoroquinolones, tuberculosis, and resistance. Lancet Infect. Dis., 3, 432–442.
5. Yew, W.W., Chan, C.K., Chau, C.H., et al. (2000): Outcomes of patients with multidrug-resistant pulmonary tuberculosis treated with ofloxacin/levofloxacin-containing regimens. Chest, 117, 744–751.
6. Aubry, A., Pan, X.-S., Fisher, L.M., et al. (2004): *Mycobacterium tuberculosis* DNA gyrase: interaction with quinolones and correlation with antimycobacterial drug activity. Antimicrob. Agents Chemother., 48, 1281–1288.
7. Cole, S.T., Brosch, R., Parkhill, J., et al. (1998): Deciphering the biology of *Mycobacterium tuberculosis* from the complete genome sequence. Nature, 393, 537–544.
8. Corbett, K.D. and Berger, J.M. (2004): Structure, molecular mechanisms, and evolutionary relationships in DNA topoisomerases. Annu. Rev. Biophys. Biomol. Struct., 33, 95–118.
9. Aubry, A., Veziris, N., Cambau, E., et al. (2006): Novel gyrase mutations in quinolone-resistant and -hypersusceptible clinical isolates of *Mycobacterium tuberculosis*: functional analysis of mutant enzymes. Antimicrob. Agents Chemother., 50, 104–112.
10. Chan, R.C., Hui, M., Chan, E.W.C., et al. (2007): Genetic and phenotypic characterization of drug-resistant *Mycobacterium tuberculosis* isolates in Hong Kong. J. Antimicrob. Chemother., 59, 866–873.
11. Groll, V.A., Martin, A., Jureen, P., et al. (2009): Fluoroquinolone resistance in *Mycobacterium tuberculosis* and mutations in *gyrA* and *gyrB*. Antimicrob. Agents Chemother., 53, 4498–4500.
12. Kim, H., Nakajima, C., Yokoyama, K., et al. (2011): Impact of the E540V amino acid substitution in GyrB of *Mycobacterium tuberculosis* on quinolone resistance. Antimicrob. Agents Chemother., 55, 3661–3667.
13. Pitaksajjakul, P., Wongwit, W., Punprasit, W., et al. (2005): Mutations in the *gyrA* and *gyrB* genes of fluoroquinolone-resistant *Mycobacterium tuberculosis* from TB patients in Thailand. Southeast Asian J. Trop. Med. Public Health, 36, 228–237.
14. Sun, Z., Zhang, J., Zhang, X., et al. (2008): Comparison of *gyrA* gene mutations between laboratory-selected ofloxacin-resistant *Mycobacterium tuberculosis* strains and clinical isolates. Int. J. Antimicrob. Agents, 31, 115–121.
15. Shi, R., Zhang, J., Li, C., et al. (2006): Emergence of ofloxacin resistance in *Mycobacterium tuberculosis* clinical isolates from China as determined by *gyrA* mutation analysis using denaturing high-pressure liquid chromatography and DNA sequencing. J. Clin. Microbiol., 44, 4566–4568.
16. Pan, X.S., Yague, G. and Fisher, L.M. (2001): Quinolone resistance mutations in *Streptococcus pneumoniae* GyrA and ParC proteins: mechanistic insights into quinolone action from enzymatic analysis, intracellular levels, and phenotypes of wild-type and mutant proteins. Antimicrob. Agents Chemother., 45, 3140–3147.
17. Lau, R.W.T., Ho, P.-L., Kao, R.Y.T., et al (2010): Molecular characterization of fluoroquinolone resistance in *Mycobacterium tuberculosis*: functional analysis of *gyrA* mutant at position 74. Antimicrob. Agents Chemother., 55, 608–614.
18. Lu, T., Zhao, X. and Drlica, K. (1999): Gatifloxacin activity against quinolone-resistant gyrase: allele-specific enhancement of bacteriostatic and bactericidal activities by the C-8-methoxy group. Antimicrob. Agents Chemother., 43, 2969–2974.
19. Malik, M., Zhao, X. and Drlica, K. (2006): Lethal fragmentation of bacterial chromosomes mediated by DNA gyrase and quinolones. Mol. Microbiol., 61, 810–825.
20. An, D.D., Duyen, N.T.H., Lan, N.T.N., et al. (2009): Beijing genotype of *Mycobacterium tuberculosis* is significantly associated with high-level fluoroquinolone resistance in Vietnam. Antimicrob. Agents Chemother., 53, 4835–4839.